



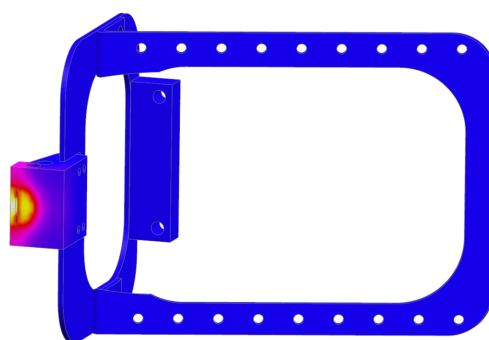
Haute école d'ingénierie et d'architecture Fribourg
Hochschule für Technik und Architektur Freiburg

Institute of industrial technologies

Mechanical Engineering Department

Academic Year 2015/2016

Bachelor Thesis Report



Design of a Mount for a new generation X-Ray Detector Board

Option	Plastics manufacturing & lightweight structures
Student	RINALDI Fabio
Supervisor	Prof. LEOPOLD Sebastian, Prof. VARNER Gary S.,
Expert Principal	WERRO Peter University Of Hawai'i at Manoa 2505 Correa Road Honolulu HI, 96822 U.S.A.
Project Number	GM_1516_P6_01_RINALDI_LEO
Date	July 29, 2016

Acknowledgements

I would like to sincerely thank:

- My supervisor in Switzerland, Prof. Sebastian Leopold, for giving me the opportunity to come at the University of Hawai'i at Manoa to realize this Bachelor thesis. thesis.
- Special thanks to my expert Mr. Peter Werro, for his valuable advice for the interest shown during the whole project.
- My supervisor at the Instrumentation Development Lab, Chris Ketter, for all his explanations about the subject and his availability.
- Prof. Gary S. Varner, for giving me the opportunity to work on a real and challenging project
- The complete team of the IDLab for the support during this project
- My family for the support shown during the studies to achieve the Bachelor

...boli te kurac...

Résumé

Le but final de ce projet était de concevoir, à partir de zéro, un support pour un capteur de Rayon-X de nouvelle génération. Une fois que le cahier des charges a été clarifié un concept simple mais fonctionnel a été établi. Ce concept a permis de comprendre la bonne direction à poursuivre pour porter en avant la conception.

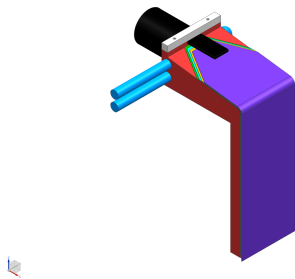


Figure 1 – Vue isométrique du concept 1.0

Ce premier concept à aussi été utilisé pour se familiariser avec les solvers NX NASTRAN THERMAL et NX THERMAL/FLOW.

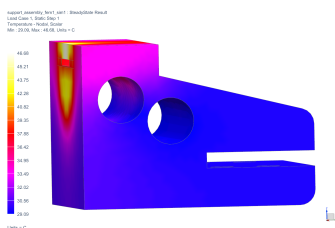
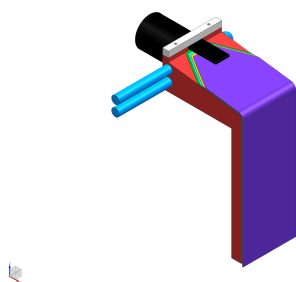


Figure 2 – Résultat de la simulation thermique faite sur le support final

La conception du support a eu lieu à différentes étapes, à chaque étape une nouvelle spécification du cahier des charges a été respectée. En parallèle la discrétisation pas éléments finis et les simulations thermiques ont eu lieu. L'interprétation des résultats des dites simulations a permis d'établir quelles étaient les dimensions et l'architecture le plus appropriées pour chaque composant. On est ainsi parvenu à avoir une structure finale avec une **masse de 379.9 g**. La dissipation de la chaleur qui se produit de l'absorption de l'énergie du Rayon-X par le support a lieu à travers un flux d'eau qui passe à travers une conduite. Le diamètre de la dite conduite a été optimisé à **6 mm** de manière de avoir un flux d'eau ($\dot{v} = 5 \text{ l/min}$) le plus turbulent possible. De cette façon il a été possible d'optimiser l'échange de chaleur entre l'eau et les parois du support.

Riassunto

Lo scopo di questo progetto era concepire, partendo da zero, un supporto per un sensore per Raggi-X di nuova generazione. Una volta messe in chiaro le specifiche richieste è stato ideato un design molto semplice che ha permesso di capire verso quale direzione indirizzare la concezione.



Questo primo design è stato anche utilizzato per familiarizzarsi con i solver NX NASTRAN THERMAL e NX THERMAL/FLOW.

Figure 3 – Vista isometrica del concetto 1.0

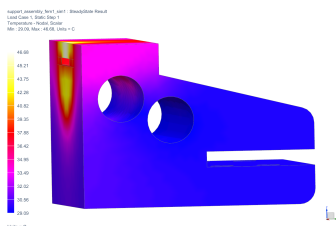
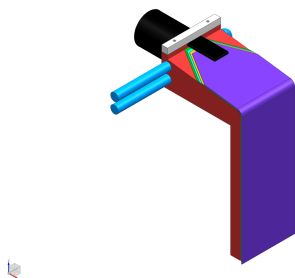


Figure 4 – Risultati della simulazione termica sul supporto finale

La concezione del supporto si è svolta a tappe, ad ogni tappa si è cercato di soddisfare almeno un punto delle specifiche richieste. In parallelo alla pura concezione, le discretizzazioni per elementi finiti e le simulazioni termiche hanno avuto luogo. L'interpretazione dei risultati di queste simulazioni ha permesso di stabilire quali fossero le dimensioni più appropriate dei vari componenti. Si è così arrivati ad avere una struttura con **massa** uguale a **379.9 g**. La dissipazione del calore generato dall'assorbimento dell'energia del fascio di Raggi-X avviene tramite una condotta per l'acqua passante due volte nel supporto principale. Il diametro di tale condotta è ottimizzato a **6 mm** in modo da avere un flusso di acqua ($\dot{v} = 5 \text{ l/min}$) il più turbolento possibile, in questo modo è possibile massimizzare lo scambio termico tra le pareti della condotta e l'acqua che vi scorre all'interno.

Abstract

The main goal of this project has been to design, starting from zero, the support for one new generation X-Ray sensor. Once the specifications have been clarified one simple concept has been designed, this concept allowed to understand in which direction the conception should go.



This concept has also been used to get familiar with the solver NX NASTRAN THERMAL and NX THERMAL/FLOW.

Figure 5 – Isometric view of concept 1.0

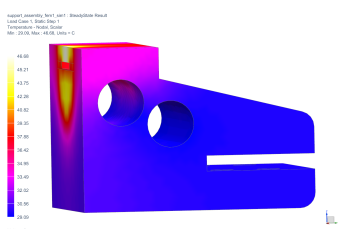


Figure 6 – Results for final support thermal simulations

The design of the mount advanced step by step, at every step one specification was satisfied. In parallel with the conception the finite element discretization and the thermal simulations take place. The interpretation of the results provided by the thermal simulations allowed to establish the proper dimensions and architecture of the whole support. The final **mass** of the support is **379.9 g**. Dissipation of heat generated by absorption of X-Ray energy by the copper support is made with water flowing through a dedicated pipe. The diameter **6 mm** and the position of the pipe have been optimized in order to have a water flow ($\dot{v} = 5 \text{ l/min}$) the most turbulent possible: in this way the heat exchange between the support and the water has been optimized.

Nomenclature

Table 1 – List of acronyms used

CAD	Computer Aided Design
FEA	Finite Element Analysis
XRM	X-Ray detector
NX	Siemens NX 10, CAD/FEA software

Table 2 – List of materials used

PI	Polyimide
Cu	Copper
Si	silicon
epoxy	epoxy resin

Table 3 – Mathematical constants

Re	Reynolds Number	-
m_s	mass of the support	kg
m_e	mass of electrical boards	kg
m_{tot}	total mass of the support	kg
\dot{v}	volimc flow	l/min
d_{min}	minimal diameter of the pipe	mm
s_{min}	minimal thickness of the shield	mm
$T_{i-support}$	initial temperature of the support	°C
Bi	Biot number	-
L_c	characteristic length of the solid	m
α	convection factor	$W/m^2 \cdot K$
λ	thermal conductivity	$W/m \cdot K$
ρ	volumic mass	kg/m^3
η	dynamic viscosity	$Pa \cdot s$
A_s	flow section	m^2

Contents

- 1 Introduction** **1**

- 2 Purpose and Approach** **3**
 - 2.1 Purpose 3
 - 2.2 Approach 3

- 3 Specifications and Conditions** **4**
 - 3.1 Design Specifications 4
 - 3.2 Simulation Conditions 5

- 4 3D Computer Assisted Design** **6**
 - 4.1 The sensor 6
 - 4.2 Analysis of the 3D model of Concept 1.0 7
 - 4.2.1 General overview 7
 - 4.2.2 Sensor position 9
 - 4.3 Concept 1.4 10
 - 4.3.1 General overview 10
 - 4.3.2 Mass 11
 - 4.4 Concept 1.6 12
 - 4.4.1 General overview 12
 - 4.4.2 Mass 13
 - 4.5 Concept 1.7 14
 - 4.5.1 General overview 14
 - 4.5.2 Mass and remarks 15
 - 4.6 Concept 1.8 16
 - 4.6.1 General overview 16
 - 4.6.2 Mass 18
 - 4.6.3 Recapitulation 18

5 Finite Elements Analysis Discretization 19

6 Simulation Conditions 23

6.1 Contacts 23

6.2 Initial thermal conditions 24

6.3 Initial Load 25

6.4 Choice of the solver 26

6.5 Simulation Time 26

7 Results 27

7.1 Simulations on concept 1.0 27

7.1.1 Without water in cooling pipe 28

7.1.2 With water in cooling pipe 29

7.1.3 Conclusion 29

7.2 Simulations on concept 1.4 30

7.2.1 Conclusion 31

7.3 Simulations on concepts 1.6 and 1.7 32

7.4 Simulation on concept 1.8 33

7.5 Conclusions 34

8 Improvements 35

8.1 Epoxy overheating 35

8.2 Global temperature 36

8.2.1 First iteration: diminution of the pipe diameter 36

8.2.2 Second iteration: changing the pipe position 38

8.3 Mass reduction 39

8.3.1 First iteration: determination of actual stiffness 39

8.3.2 Second iteration: creating the new model and simulation 41

9 Conclusions 42

9.1 Synthesis and final design 42

9.2 Recommandations 43

Appendices	46
A Calculations	46
A.1 Heat Transfer	46
A.2 Flow Characteristics	47
A.3 X-Ray penetration in the matter	48
A.4 couple on the rotational stage	48
B Positioning motors data-sheets	49

Chapter 1

Introduction

This introduction is intended to introduce someone who is not familiar with High Energy Physics and Engineering into the main topic of this Bachelor Thesis. The *Belle Corporation* is leading the Belle Experiment in Tsukuba, Ibaraki Prefecture in Japan, more than 400 physicists and engineer are investigating the effects of collisions between small particles (*electrons and protons*) in the *High Energy Accelerator Research Organisation* (KEK). Like in the *Large Hadron Collider* situated at the *CERN site in Geneva* the KEK, in the fig. 1.1 we find a simplified schematics of the actual installation, facility is composed by two main rings where the particles are accelerated with electrical energy and kept in a circular trajectory thanks to big electromagnets that make the particles turn in the decided direction. During the experiment X-Ray beam are generated, the detector which is the core and the motivation of this bachelor thesis will have the task of characterizing the *beam composition*.

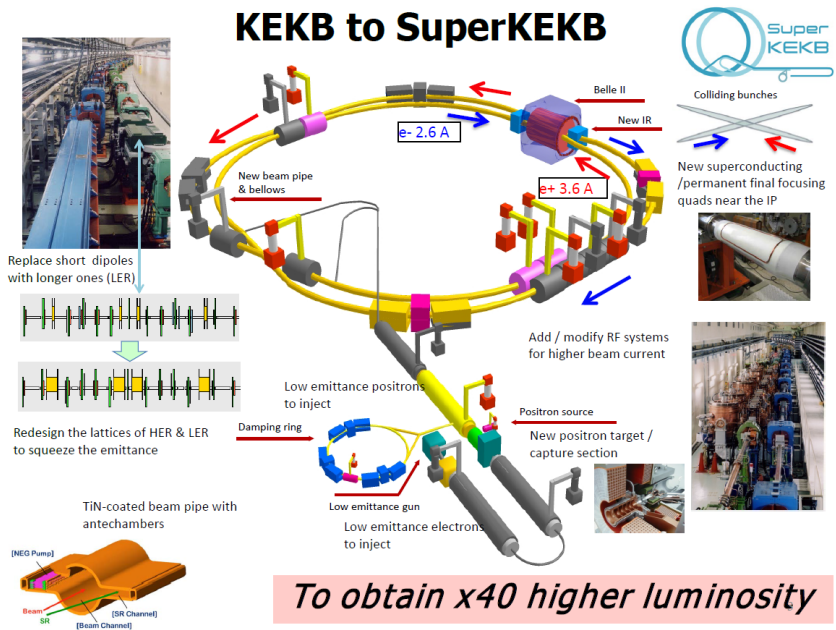


Figure 1.1 – KEK facility layout

In order to understand what composition means it is helpful to know that a typical beam is not a continuous flow of particles, it is better to imagine it like packages of particles come one after the other in variables time spans - normally $4\ \mu\text{s}/5\ \mu\text{s}$ or 0.00004 seconds, yes it is really fast but not continuous! - other that the time constrain the particles packages are not always fulfilling the area of the beam. In the case of this project the beam has a diameter of $15\ \text{mm}$ and a cross section of $177\ \text{mm}^2$, the packages will pass through this section and their position will be aleatory; the sensor will serve to detect where and what is flowing through the beam section. In order to fulfil his mission the sensor has to be put in the conditions of inspecting the whole beam cross section: two translational and a rotational stages will make this possible. The whole support will be placed in a sealed box and the box will be fulfilled with Helium Gas to prevent the beam to badly interact with air and the particles presents there. A typical experimenting routine will start with the activation of the X-Ray beam source, then the sensor will come in position and his center will be placed in the exact center of the beam using the two translational stages (up-down and left-right regulations), once the sensor is in position it can start acquiring data, if needed the rotational stage allows to turn the sensor in order to inspect the whole beam area. At this point the most logical question is: *What the sensor really is?* well, the sensor is composed by 128 tiny copper wires bonded one parallel to the other and glued on a silicon wafer, the beam should pass in those wires perpendicular to their cross section. To visualize it imagine a sharpshooter shooting at his target, surely he can got good results shooting from the side of the target but he will achieve the best results when he is perfectly perpendicular to the target, or not? In the same way the X-Ray beam will be characterized at his best when the beam passes through the cross section of the wires and runs through their entire length. For this reason the starting position of the sensor is vertical and from this configuration the design of the mount will start. The design will not be limited to the mount but it will be necessary to think where to actually put the electronic devices that it needs to work properly. Many conditions will be affronted during this project the overheating of the devices and the danger of the radiations and their penetration in the matter are the most interesting among the others.



Figure 1.2 – The X-Ray entering the box through an orifice, side note: the picture has been taken without external light source...

Chapter 2

Purpose and Approach

2.1 Purpose

The main purpose of this project was to imagine and design a support for a new generation X-Ray sensor and the electronics board that makes the sensor work. Once a rough design has been established it has been simulated for displacements (to reduce and optimize the mass) and heat transfer in order to judge if a water cooling installation was necessary or not.

2.2 Approach

To accomplish the goal of this project the following steps have been followed:

- Establishing the Design Specifications
- Preparing a simple design to get used to the main problems with Heat Transfer simulations
- Design and simulations of the first concept
- Adjustments and calculations (heat transfer, flow nature, Re ,...)
- Interpretations of the first results
- Improvement of the concept with new elements (electronic boards and different piping)
- Improvement of simulations
- Interpretation and possible improvements
- 2D fabrication sheets

Chapter 3

Specifications and Conditions

The Design Specifications and the Simulation Conditions evolved along the project. The list below resumes all the specifications that have been required from the beginning until the end of this bachelor thesis.

3.1 Design Specifications

- **Mass** the mass of the ensemble (mount, sensor, electronics) is limited to **1 kg**
- **Protection** it is mandatory to protect the **electronic boards** from the X-Ray beam
- **Temperature** keep the temperature as low as possible, the sensor maximal working temperature of **150 °C**
- **Centering** the sensor has to be placed on the axis of rotation of an existent rotational stage
- **Security** both the rotational and translational stages have to be safe from direct radiations
- **Dimensions** the ensemble has to be smaller than **400x400x120 mm**
- **Cables** to avoid the most signal noise possible the length of the cables has to be **minimal**
- **Symmetrical** since there are two similar installation the same mount must be **mountable on both** of them

3.2 Simulation Conditions

In the list below the principal simulation conditions are listed. Once the support fabricated it will take place in a closed box and the beam will pass through an orifice and hit the sensor.

- **Water Flow:** the water flow available is $\dot{v} = 5 \text{ m/s}$
- **Water Temperature:** the water temperature has been estimated to **T=20-25°C**
- **Pressure:** the pressure in the water pipes is **0.15 MPa**
- **Pipe Size:** the pipe in the installation has a diameter of $d_{\text{max}} = 0.5 \text{ Inch} - d_{\text{max}} = 12.7 \text{ mm}$
- **Environment:** the mount will take place in a closed box, **without free air flow**
- **Controlled Atmosphere:** in order to prevent/limit scattering of the X-Ray beam the box will be fulfilled with **Helium**
- **X-Ray Beam Size:** the beam will have a diameter of $d_b = 15 \text{ mm}$
- **Heating Power:** the heating power is approximated to a heat flux: $\dot{q} = 1 \text{ W/mm}^2$
- **Time:** since the experiment could be running for days the time limit is a little above the equilibrium time constant of the system

In the Figure 3.1 it is possible to see a picture of the actual installation, the walls of the box are visible as well as the inlet orifice.

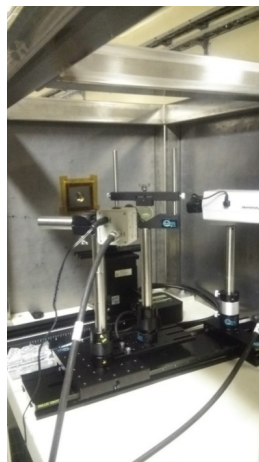


Figure 3.1 – Overview of the actual installation

Chapter 4

3D Computer Assisted Design

In this chapter the principal concepts that lead to the final results will be shown and explicated. As new informations/specifications were provided the concept has been adapted to fit them in the most efficient and simple design possible. Not every concept is shown and described in this chapter, the initial model and the 4 main concepts are shown and described, at every step new specifications were included in the design.

4.1 The sensor

Before starting with the mount design it is necessary to acknowledge the geometry, the sizes and the particularities of the sensor. In the Figure 4.1 it is possible to see the sensor layout, as it is possible to observe the real sensor is composed by 130 different strips of copper. The sizes of the active device are finally: $6750\ \mu\text{m} \times 2415\ \mu\text{m} \times 75\ \mu\text{m}$, the X-Ray beam will be hitting the $6750\ \mu\text{m} \times 75\ \mu\text{m}$ section and the sensor will work positioned in vertical.

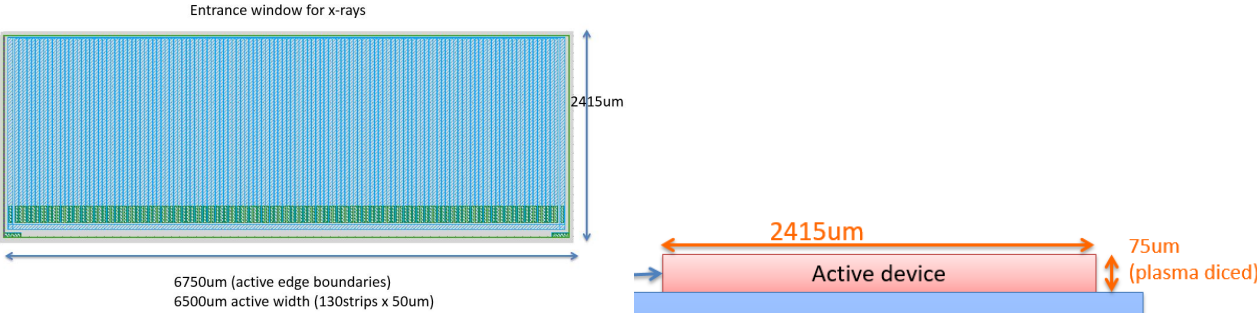


Figure 4.1 – Sensor layout and dimensions

In order to simplify the CAD and FEA simulations the sensor has been designed as a unique copper parallelepiped, in the Figure 4.2 the 3D model is shown. Like the real device the dimensions are $6750\ \mu\text{m} \times 2415\ \mu\text{m} \times 75\ \mu\text{m}$

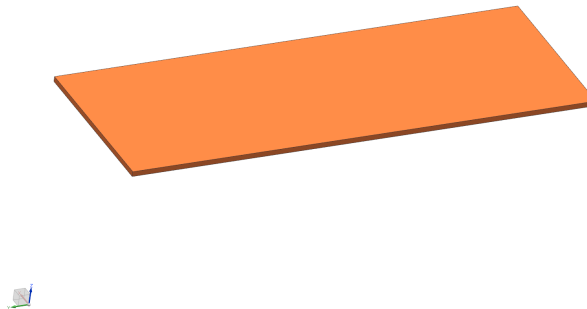


Figure 4.2 – Sensor 3D model

4.2 Analysis of the 3D model of Concept 1.0

The concept 1.0 has been used primarily to understand in which direction the design should go: some dimensions are empiric and will be adjusted in the following chapters.

4.2.1 General overview

In order to fully understand the model it is necessary to be familiar with the following design names:

- the red solid is the actual support, the chosen material is copper¹
- the black cylinder is representing the X-Ray beam hitting the support
- the black parallelepiped is representing the portion of the beam passing the sensor
- the blue tube is representing the cooling pipe
- the white bar is a security shield for the electronic boards, it is of the same material of the support
- the green, light-blue, orange and purple elements are representing the flexible cables relying the sensor and the pre-amplifiers stage

¹Been known for the processing ease and the thermal properties copper has been chosen for the first designs and simulations

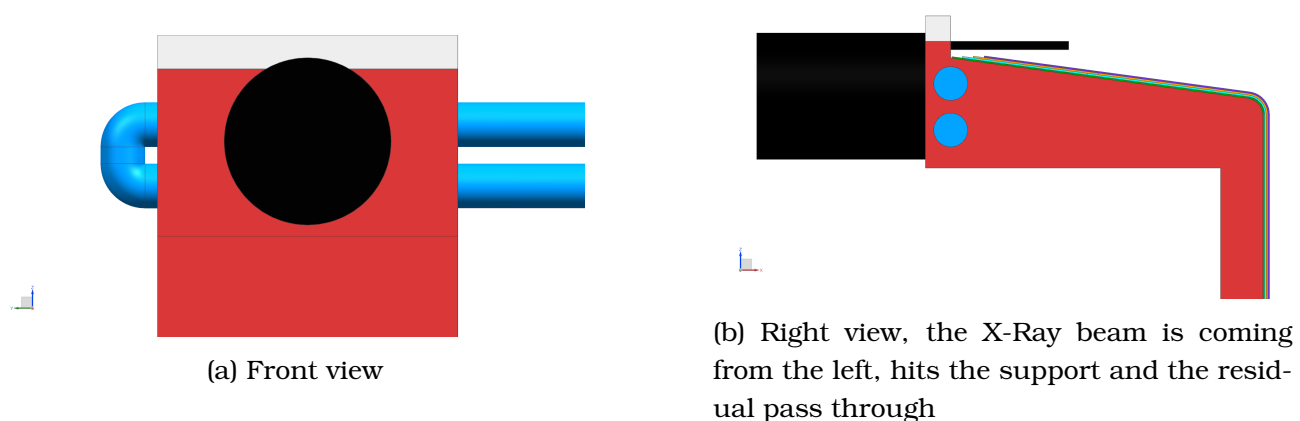


Figure 4.3 – Overview of the support of the concept 1.0

The choices of the support's geometry are made in order to keep the electronics boards out of the beam action area, in the Figure 4.3 it is possible to see how with an inclined plane the flexible cables are driven away from the beam remains. The flexible cables are composed by PI and copper, the thickness is the lowest that can be found on the market: $200\ \mu\text{m}$. Since the bending limits of cables are known, the minimal bending radius is defined by the following formula:

$$r = \textit{thickness} \cdot 10 \quad (4.1)$$

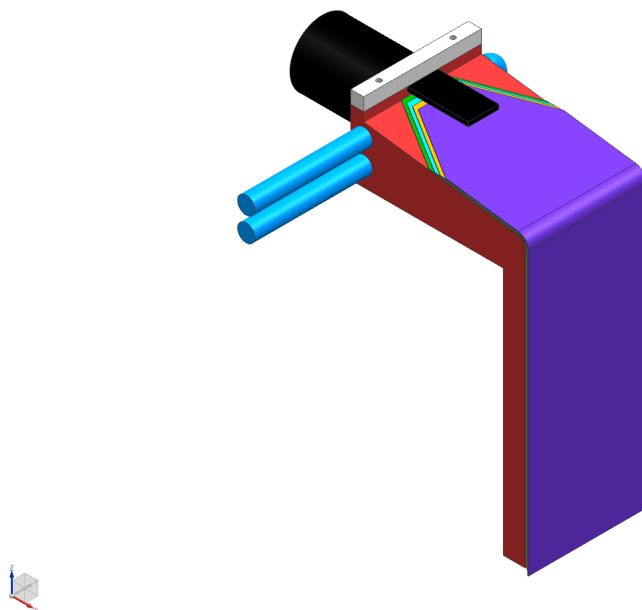


Figure 4.4 – Isometric view of the first concept

4.2.2 Sensor position

The active device is bonded to a silicon wafer², afterwards the silicon wafer is bonded with a layer of epoxy³ to the support.

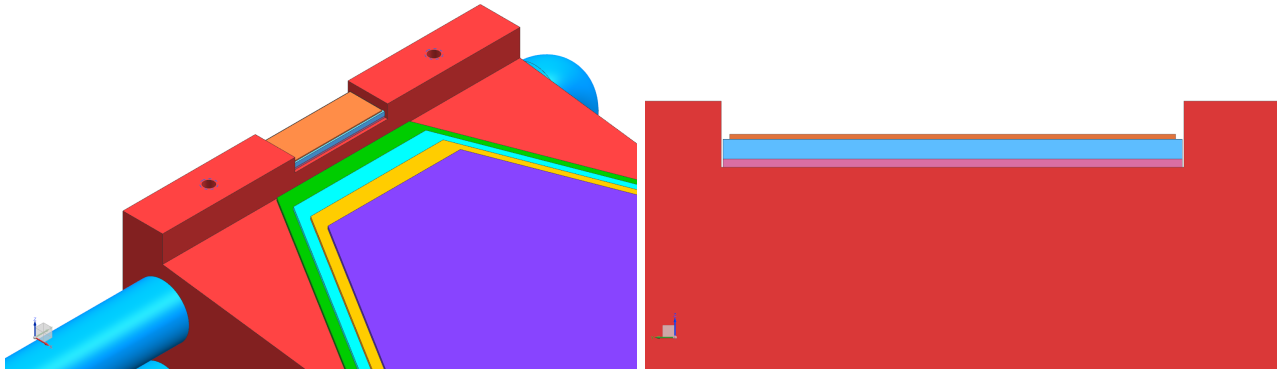


Figure 4.5 – Sensor position

Once the whole support assembled and mounted the sensor will work in a vertical position. As it can be seen in the Figure 4.6 the X-Ray beam is not completely hitting the device: the position of the beam at this stage of conception is aleatory but it will be clarified and explicated in the development of the project.

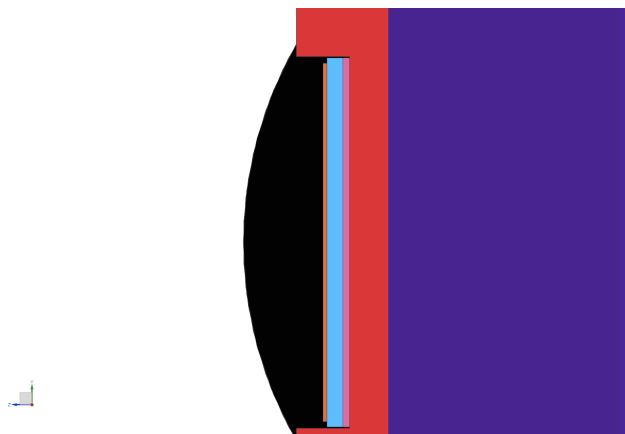


Figure 4.6 – Sensor in working position

²Dimensions 6950 μm x 2615 μm x 300 μm , blue block in the Figure 4.5

³Estimated thickness = 125 μm , rose parallelepiped in the Figure 4.5

4.3 Concept 1.4

4.3.1 General overview

In the concept 1.4 the rotational stage which will regulate the orientation of the sensor and a first half of the electronic board make their appearance. As it is possible to see in the Figure 4.7 the rotational stage is represented in black and the electronic part is divided between the amplifiers in red and the SCROD board in blue. The black cylinder is representing the X-Ray beam.

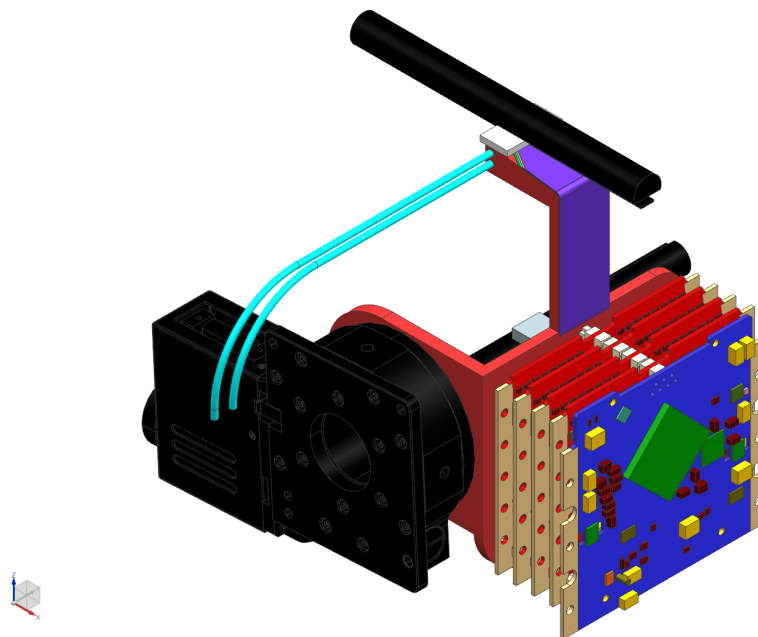
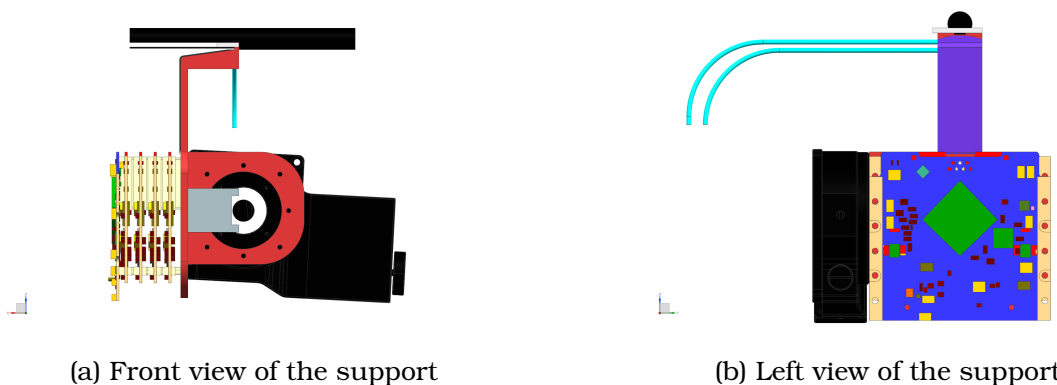


Figure 4.7 – Isometric view of concept 1.4

In order to respect the constrain **protection** both the rotational motor and the electronics have been placed away from the beam:



(a) Front view of the support

(b) Left view of the support

Figure 4.8 – Front and right views of the concept 1.4

4.3.2 Mass

The mass of the support has been determined with the NX FEM "Solid Properties Check" command and it is: $m_s = 535.8$ g. Since the support is not yet complete (the pre-amplifiers are not incorporated in the design) In this configuration it is important to start thinking about the mass that will be added to the mount: the 4 amplifiers board and the SCROD have therefore been weighted: the combined mass of the 5 elements and the connectors is: $m_e = 483.9$ g. In the Figure 4.9 the method used to determine the mass is shown, the balance used is old but very precise and effective.



Figure 4.9 – Mass determination of 2 amplifier boards

The total mass is now $m_{tot} = m_s + m_e = 1019.7$ g, it clearly overpass the **mass** specification but at the moment it has been decided that is more important to provide a simple concept with a working thermal simulation. The mass problem will be approached in the Chapter 8 where the stiffness of the mount will be judged.



Figure 4.10 – Details of the balance, precision stated at **0.1 g**

4.4 Concept 1.6

4.4.1 General overview

Due to the **centering** specification the sensor (and the X-Ray beam!) has to be moved closer to the rotational stage, this implies major changes in the design. Moreover the sensor orientation has to be vertical: as explained in the Chapter 1, the testing routine and the following **security** specification lead to this orientation of the sensor. In the Figure 4.11 it is possible to see the trimetric overview of the 1.6 design:

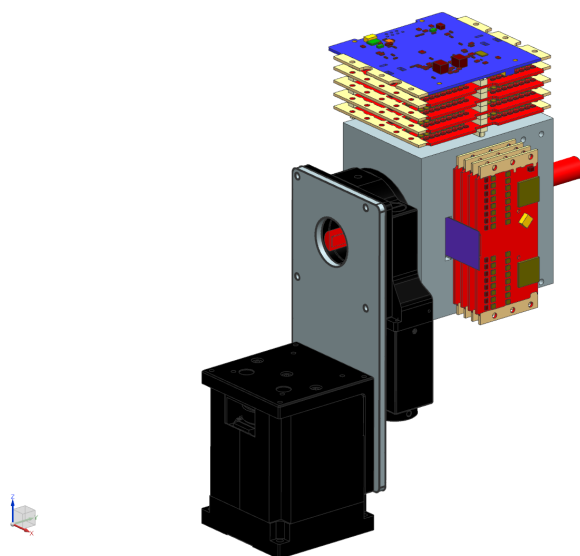


Figure 4.11 – Trimetric view of concept 1.6

In this concept the **X-Ray beam** is represented by a **red cylinder**. The vertical translational stage (black parallelepiped) has also been added to complete the whole installation, the flange relying the two motors is not part of the design since is already present and will be used in the future.

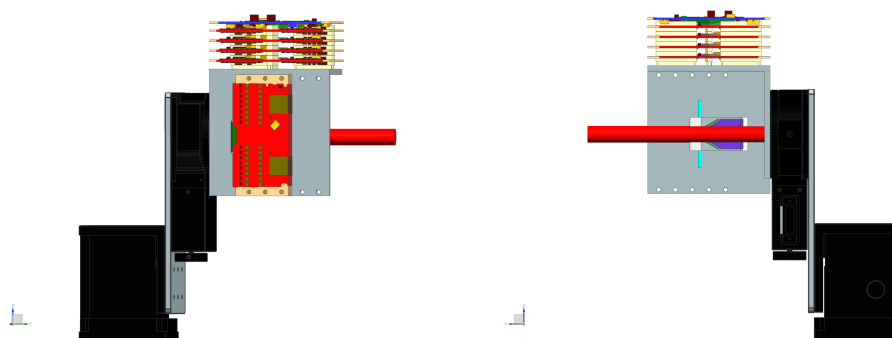


Figure 4.12 – Left and right views of the concept 1.6

Another issue that came up with this concept is the necessity of a direct and as shortest as possible connection between the pre-amplifiers and the amplifiers stages, this means that the 8 boards need to be on the same plane, therefore on the same mounting plate and not on perpendicular planes as it can be observed in the Figure 4.12.

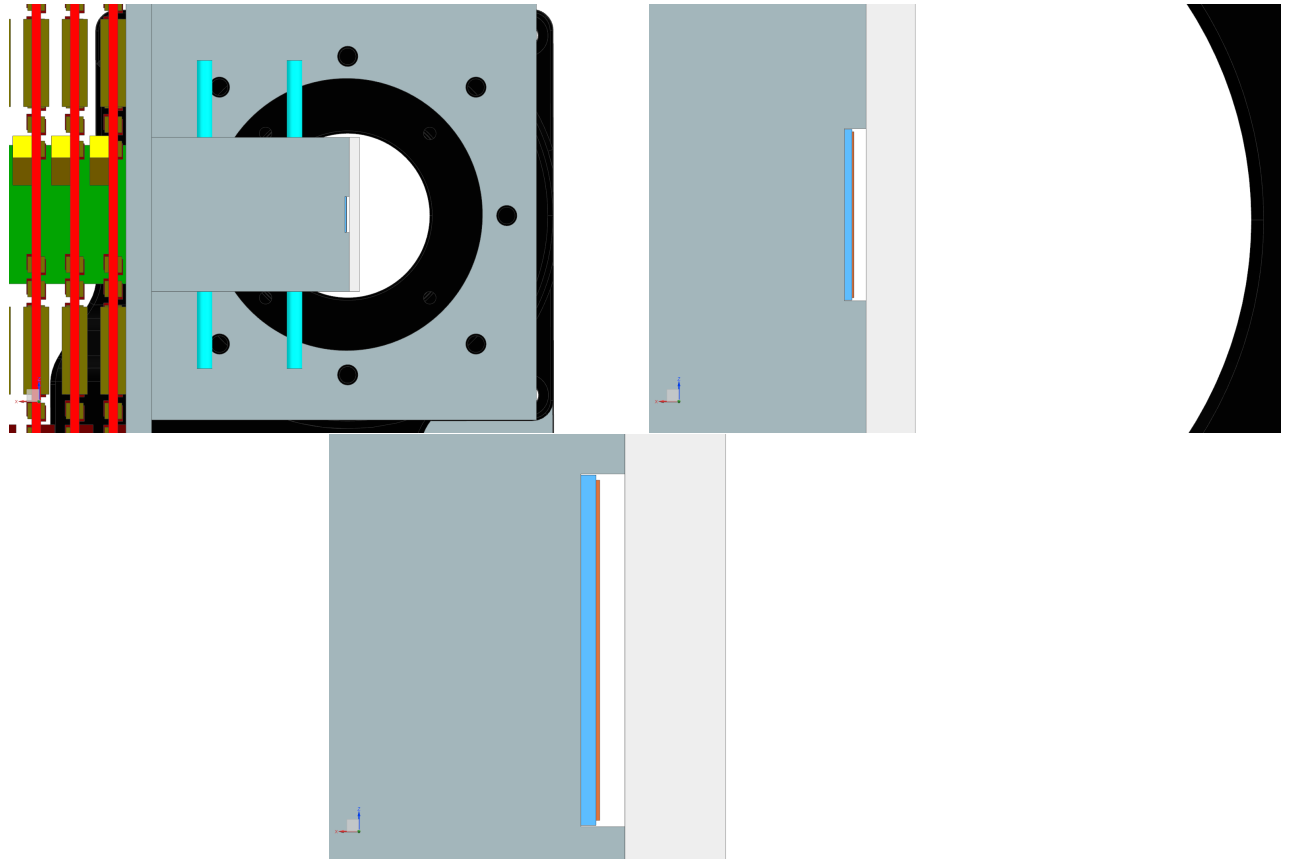


Figure 4.13 – Sensor position

The Figure 4.13 shows the sensor emplacement and the sensor itself, it is possible to observe how the sensor has really small dimensions in relation to the rest of the ensemble.

4.4.2 Mass

The mass of this concept, without the electronic boards is $m_s = 1583.2$ g, with the complete electronic installation (pre-amplifiers, amplifiers, SCROD and connectors) it is $m_{tot} = 2202.3$ g which is more than the double than allowed by the **mass** specification. The following concepts absolutely to decrease the mass.

4.5 Concept 1.7

4.5.1 General overview

In the concept 1.7 the orientation of the rotating stage changed, due to the lack of space for the cables on the bottom, the stage has been flipped with the command cables coming from the superior part, the new orientation of the rotational stage can be seen in the Figure 4.15(b), in this same Figure the output of the cables is visible, at the top of the motor. This requirement involved the creation of a shield thick enough to protect the cardboards from an accidental beam hitting them, according to the Appendix A.3 the minimal thickness is: $s_{min} = 5 \text{ mm}$.

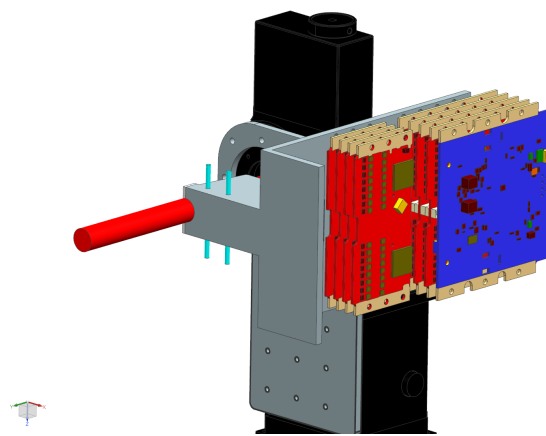
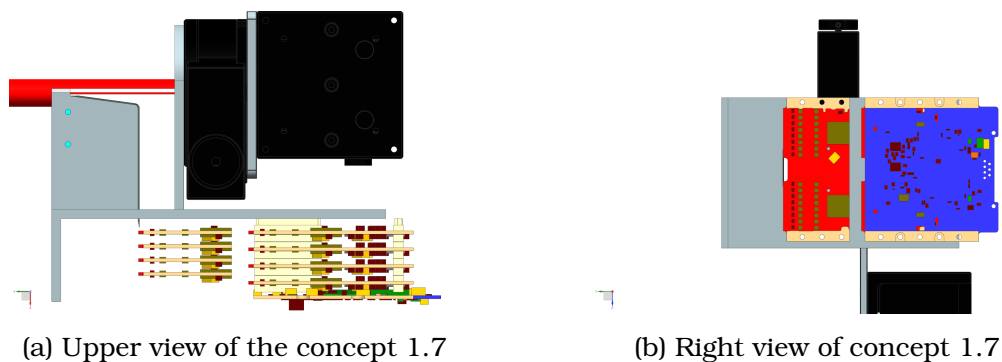


Figure 4.14 – Isometric view of 1.7 concept

In the upper view from the Figure 4.15(a) it is possible to see how in this concept the 8 boards are aligned and a straight and short connection is easily feasible. The shield protecting the boards it is also visible on the left of that Figure.



(a) Upper view of the concept 1.7

(b) Right view of concept 1.7

Figure 4.15 – Upper and right views of the concept 1.7

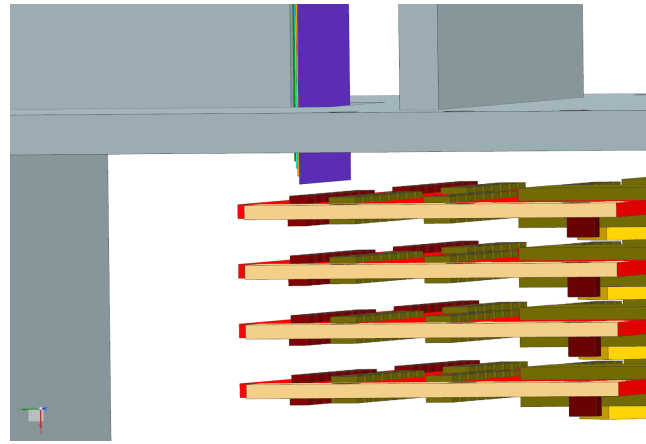


Figure 4.16 – Flexible cables for signal transmission

In the Figure 4.15(b) it is possible to see how the boards are not centered in rapport to the rotational stage. This geometry has been chosen because of the cables coming from the sensor and joining the pre-amplifiers: in the Figure 4.16 the output cables coming from the sensor and passing through a pocket in the mount are visible.

4.5.2 Mass and remarks

The mass of the support in this configuration is $m_s = 2138.6$ g and the combined mass of the complete installation is now $m_{tot} = 2757.7$ g, roughly **2.7 times the mass allowed** by the specifications! Furthermore the cables that transmit the signal from the sensor to the pre-amplifiers is now between **100 mm** and **112 mm**, this length is excessive and needs to be shortened as much as possible.

4.6 Concept 1.8

At this point of the designing process the *Design Specifications*⁴ list is complete and known; the concept 1.8 is supposed to fulfil the requirements.

4.6.1 General overview

In order to minimize the length of the cables this concept assumes a "dihedral" shape, as is it shown in the Figures 4.17 and 4.18 the plate where the electronic boards are fixed is inclined toward the rotational stage. The inclination is enough to keep the length of the cables between **49 mm** and **51 mm** but a complete revolution of the mount around the axe of rotation of the motor is still possible, if necessary.

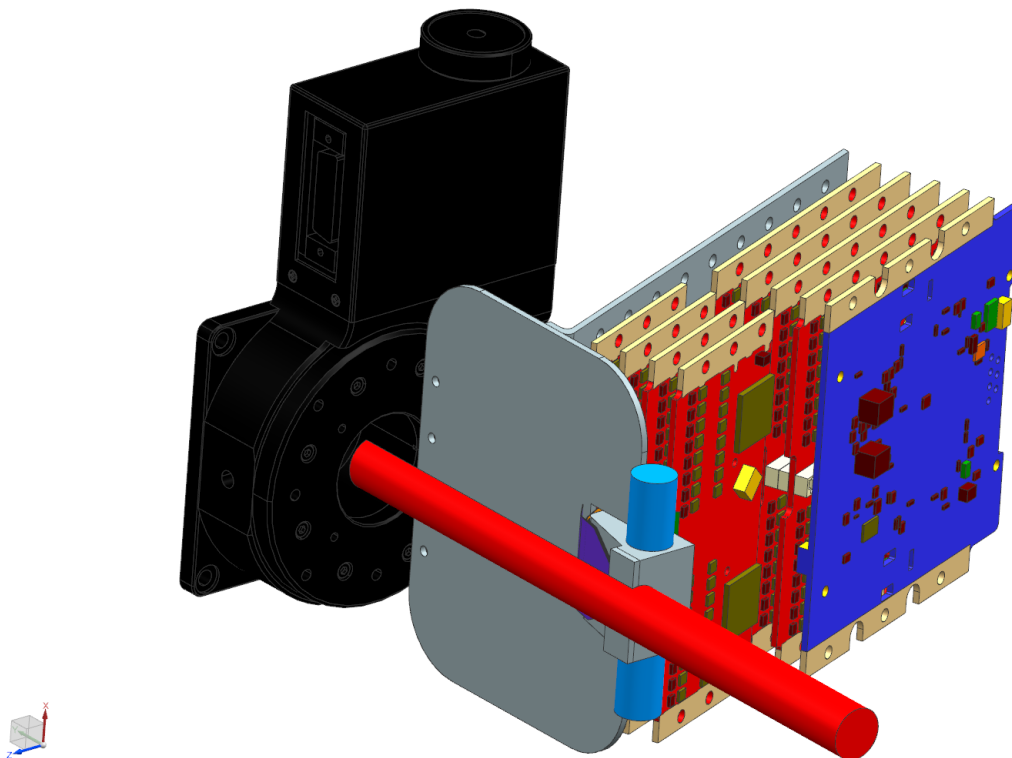


Figure 4.17 – Isometric view of concept 1.8

⁴Refer to Chapter 3.1

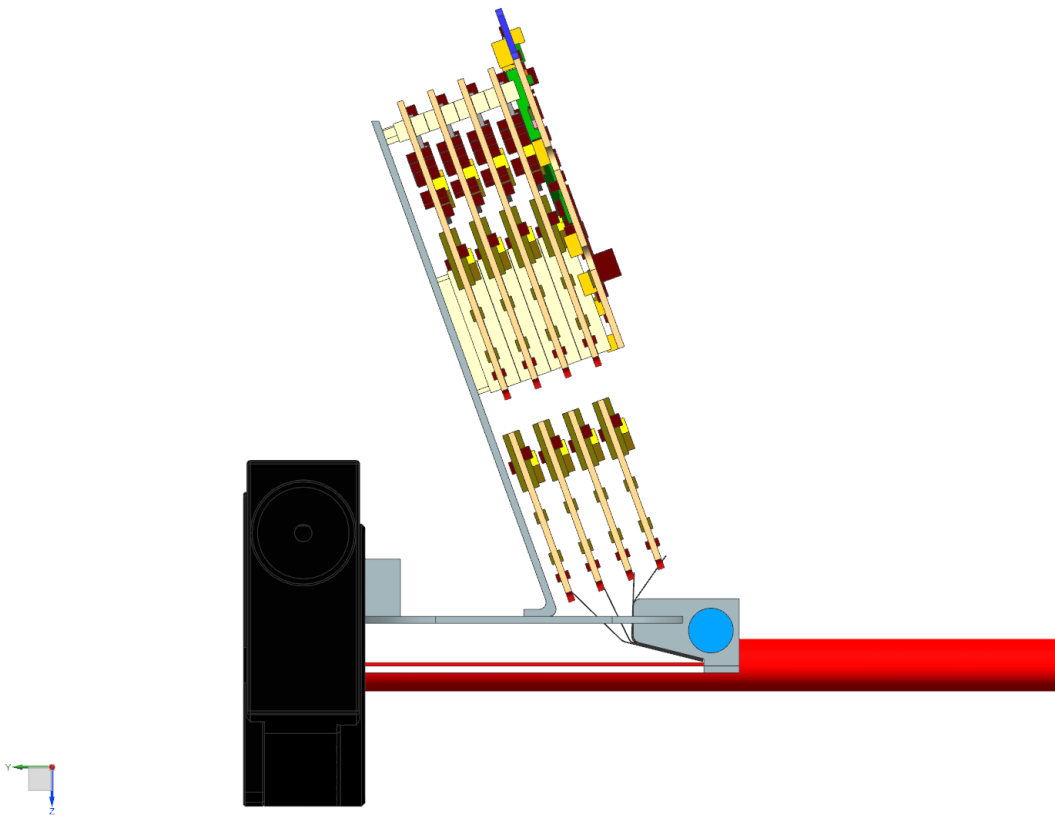


Figure 4.18 – Upper view of concept 1.8

In relation to the previous concepts where the pipe had a minimal diameter of $d_{\min} = 3 \text{ mm}$ in this concept the diameter is increased to the max value of $d_{\max} = 12.7 \text{ mm}$. This change is due to the small size of the support of the active device, putting the biggest pipe possible leave enough space for small and fast changes in dimensions and position. One other difference with the other concepts it is that if the others were realisable from one piece of copper this one instead it has been divided in 4 different corps (two plates, one flange and the actual support of the sensor); as it will be shown in the Chapter 8 this feature give the possibility to easily use different materials in order to make the structure more lightweight and more rigid. The single flange which serves to connect the support to the rotational stage allows it to be mounted on the other side as well, the **symmetrical** specification is hence satisfied

4.6.2 Mass

The mass of this support is $m_s = 664.8$ g which gives a total mass of $m_{tot} = 1283.9$ g. The weight reduction is mainly due to the change of architecture and the subsequent shrinking of the actual support part which is not massive as it used to be. In the Figure 4.19 it is possible to see the difference between the concept 1.7 support (Figure 4.19(a)) and the support from the concept 1.8 (Figure 4.19(b)).

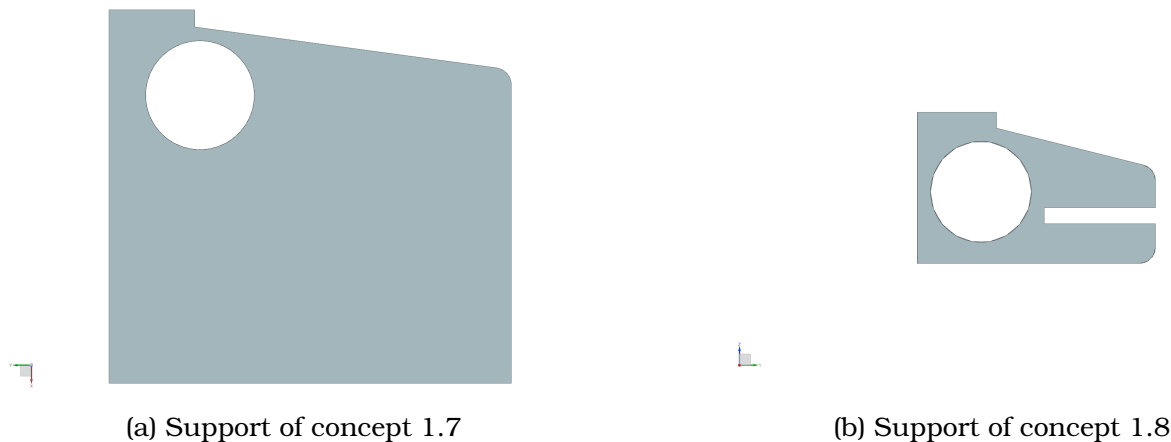


Figure 4.19 – The two active device supports, the hole has the same size: $d_h = 12.7$ mm

The mass of the support of the 1.7 concept is $m_s = 542.9$ g and the mass of the support of the 1.8 concept is $m_s = 83.4$ g, a mass reduction of nearly **85%**.

4.6.3 Recapitulation

- **mass:** to satisfy this specification a 22% mass loss is still required
- **protection:** the electronic boards are away from the beam, it is possible to easily add a shield if needed
- **centering:** the sensor is positioned perfectly centered with the axis of rotation
- **security:** the beam passes exactly through the hole in the rotational stage, in case of important translation (more than 5 mm) a shield is needed
- **dimensions:** with the dimensions of 188x115x106 mm the specification is satisfied
- **cables:** the cables and connections are the shortest possible
- **symmetrical:** the support can be mounted on both sides of the rotational stage without any problem

Clearly one of the most important specifications, the **temperature**, can not be judged in this chapter, the thermal simulations of the Chapter 6 will clarify where it is necessary to focus the efforts in order to optimize the heat dissipation.

Chapter 5

Finite Elements Analysis Discretization

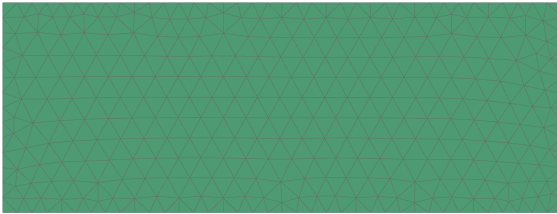
In this chapter the choices made during the discretization of the different components will be briefly explicated. With the necessity of knowing the heat transfer in the 3 dimensions of the ensemble, the choice of the **3D tetrahedral elements** in **10-noded elements** has been preferred over the **3D hexahedral** due to the different geometries making the support. The choice of the dimensions of the single element has been determined after many attempts: meshing the single piece was not difficult but the creation of the **mesh mating** or the **Surface-to-surface contact** were not precise at all and sometimes the results were not linear nay the results were not homogeneous between two different pieces. Finally, especially for the smallest components (sensor, silicon wafer, epoxy) it has been chosen to use their **minimal thickness as element size**. Not all the elements of the 3D design are been used for the FEA, here follows the list of the components used:



Active device of the sensor, element size:
0.075 mm, 41427 nodes, 20368 elements,
material copper



Figure 5.1 – Mesh of the sensor



Wafer, element size: 0.3 mm, 5885 nodes,
2740 elements, material silicon



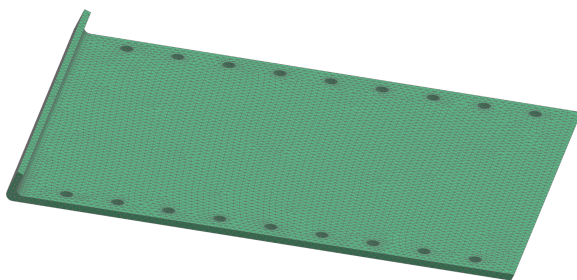
Figure 5.2 – Mesh of the wafer



Epoxy layer, element size: 0.125 mm, 11005
nodes, 5128 elements, material epoxy



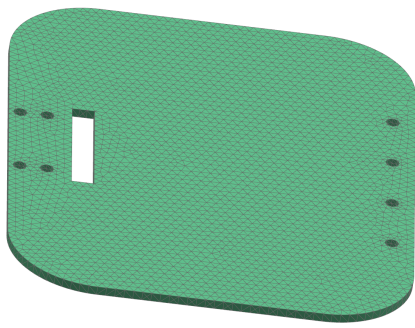
Figure 5.3 – Mesh of the epoxy layer



Electronics support, element size: 2 mm,
71247 nodes, 35369 elements, material
copper



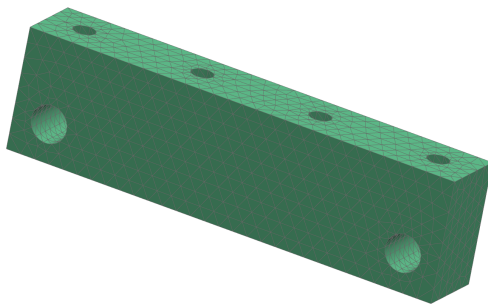
Figure 5.4 – Mesh of the support for the electronic boards



Plate, element size: 2 mm, 36925 nodes,
18108 elements, material copper



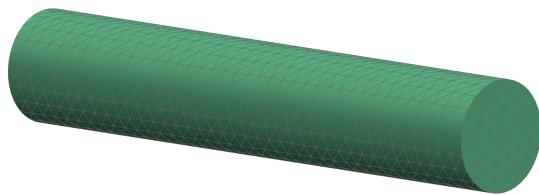
Figure 5.5 – Mesh of the plate



Plate, element size: 2 mm, 15479 nodes,
9302 elements, material copper



Figure 5.6 – Mesh of the flange

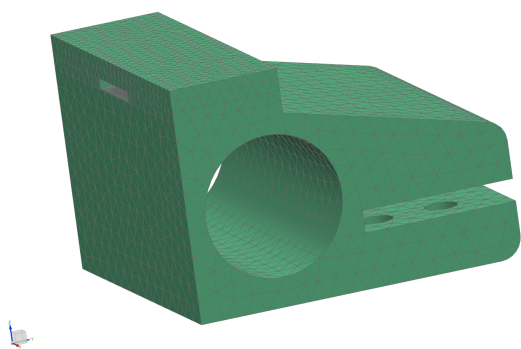


Internal pipe, element size: 2 mm, 9163
nodes, 5394 elements, material water



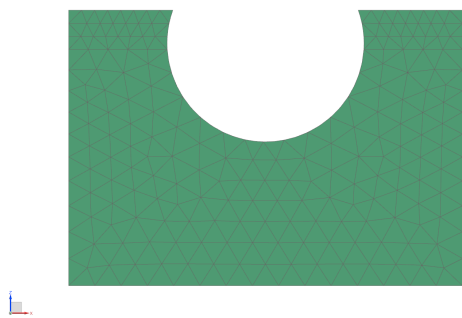
Figure 5.7 – Mesh of the internal diameter of
the pipe

The discretization of the support of the active device has been done in several elements. In order to generate the proper conditions for the application of the heat flow during the simulation it has been necessary to divide the body of the support with a cylinder having the same diameter of the beam: $d_b = 15 \text{ mm}$. In the Figure 5.8 the complete mesh of the support with his characteristics is shown and in the Figure 5.9 the body division is represented. This division of the support generated many smaller bodies that have been meshed separately, anyway in the Figure 5.8 the a summary of the complete support is presented.

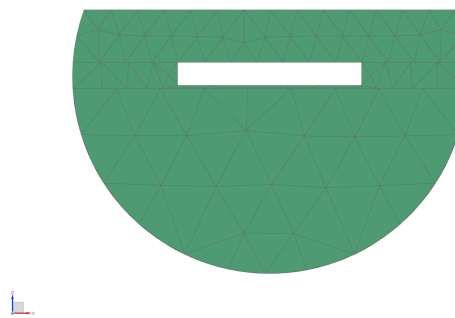


Plate, element size (variable): 0.125-1-2 mm, 41683 nodes, 22787 elements, material copper

Figure 5.8 – Mesh of the active device support



(a) Mesh of the body without the beam



(b) Mesh of the beam

Figure 5.9 – Subdivision of the support, in order to separate the beam action area

Once the different meshes have been created the **Mesh Mating** condition between the different bodies is created and activated. At this point the mesh is complete and ready to be used for the simulations.

Chapter 6

Simulation Conditions

In this chapter the **Boundary and Initial Conditions** used to simulate at the best the heat transfer in the support will be explained.

6.1 Contacts

In order to improve the results it has been necessary to establish several **Surface-to-Surface Contact** type contact conditions. In the Figure 6.1 those contacts are highlighted by dark yellow symbols:

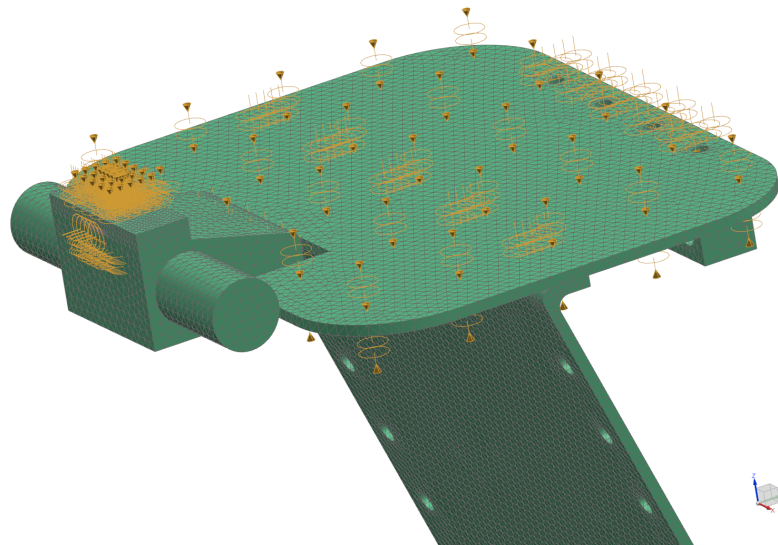


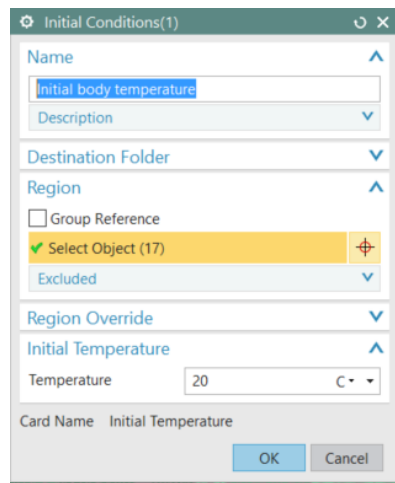
Figure 6.1 – Simulation Contacts between surfaces

There are 14 different contact between surfaces, obviously the zone with the most surfaces is the support where the active device is: contact between the support and the epoxy, the epoxy and the wafer, the wafer and the sensor,...

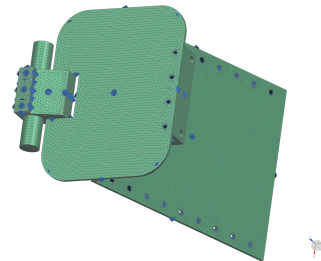
6.2 Initial thermal conditions

The initial condition applied is the initial temperature at which the solid body is:

$$T_{i\text{-support}} = 20\text{ }^{\circ}\text{C}.$$



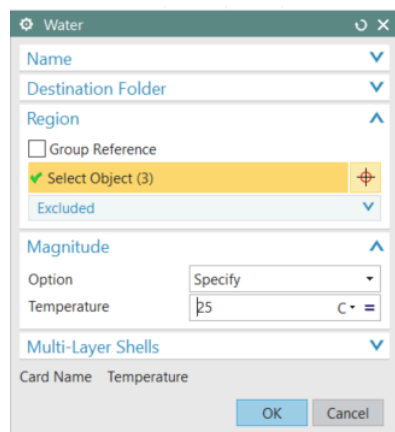
(a) Initial body temperature window



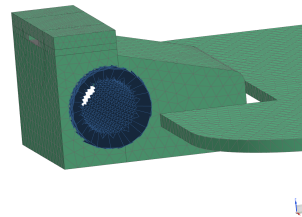
(b) Blue symbols of temperature on the mesh

Figure 6.2 – Application of the initial temperature to the complete support

Since the first simulation did not take in count the heating of the water flow, the temperature of the water has been set as constant at $T_{c\text{-water}} = 25\text{ }^{\circ}\text{C}$. In the Figure 6.3



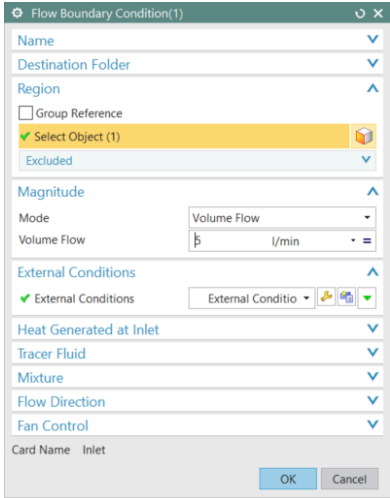
(a) Initial water temperature window



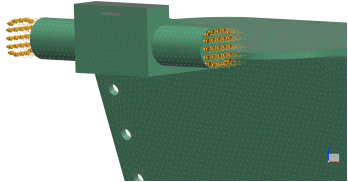
(b) Blue symbols of temperature on the mesh

Figure 6.3 – Application of the initial temperature to the water

When the simulations took in count the actual water flow and the heating, the initial water temperature has been set to $T_{i\text{-water}} = 25\text{ }^{\circ}\text{C}$. To complete the water flow characteristics it has been mandatory posing the volume water flow which is: $\dot{v} = 5\text{ m/s}$. Those conditions can be seen in the following Figure 6.4.



(a) Initial water flow/temperature window

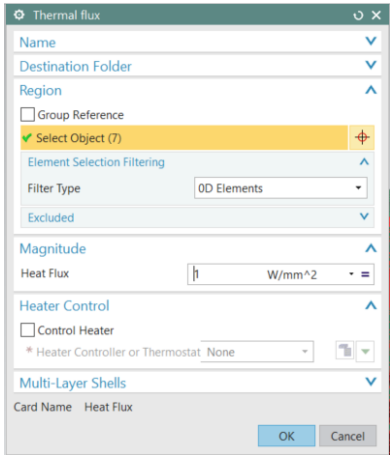


(b) Dark yellow symbols of the water flow

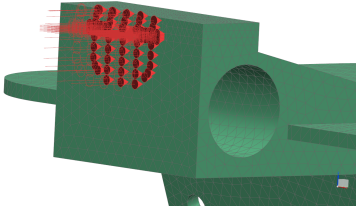
Figure 6.4 – Application of the initial temperature and initial flow volume rate to the water

6.3 Initial Load

The heating power that the X-Ray beam will transmit to the support is $\dot{q} = 1 \text{ W/mm}^2$ which with the beam diameter $d_b = 15 \text{ mm}$ is equivalent to 176.7 W . Instead of calculating the exact amount of power to apply to every single element it has been decided to apply the heating flux to the areas involved: the support, the epoxy layer, the silicon wafer and the sensor. In the Figure 6.5 it is possible to see the load conditions and the load command window:



(a) Heating flux load



(b) Red arrows representing the flux load

Figure 6.5 – Application of the heat flux as load

6.4 Choice of the solver

The first solver used is the **NX Nastran THERMAL**, this solver is very simple and does not allow the simulations of fluids, therefore the very first simulations has been done with the water constant temperature as shown in the Figure 6.3. This solver provided has been abandoned since the simplification that the water keeps the same temperature during the passage in the pipe was not acceptable. The demand of accuracy lead the choice to the **NX THERMAL/FLOW** solver where with a **coupled analysis thermal/flow** it has been possible to simulate the actual temperature of the water and be more precise with the simulations. The initial and boundary conditions of the flow can be found in the Figure 6.4.

6.5 Simulation Time

The time of the simulation vary in rapport to the boundary conditions, number of contacts,... the conditions presented in this chapter lead to a *Steady State Simulation* that requires roughly 7 min and 30 s. For a *Transient Simulation* with enough precision (2 steps every second, $t=2000$ s) the simulation time exceeds the 4 h. The choice of the "limit" time at $t=2000$ s is explicated in the Appendix A.1, this time is called the equilibrium constant of the system and represents the time at which the system is in equilibrium, namely when the temperature of the system is perfectly constant.

Chapter 7

Results

This chapter is dedicated to show and describe the evolution of the different simulations.

7.1 Simulations on concept 1.0

In the following sections the simulations with and without cooling devices lead to the decision to effectively use some cooling pipes. The solver used for these simulations is the *NX NASTRAN THERMAL*.

7.1.1 Without water in cooling pipe

This simulations without any cooling device has been made to understand at which temperatures would the support, and specially the sensor, arrive once the steady state of the system is reached.

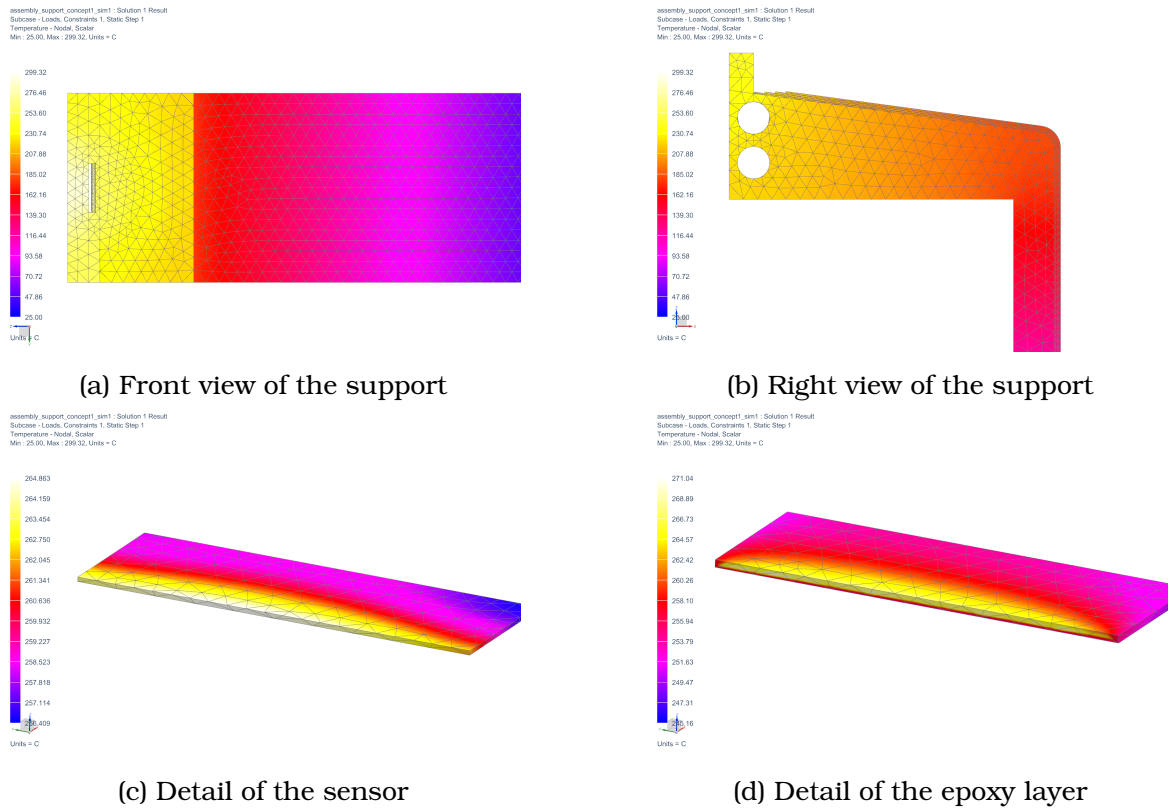


Figure 7.1 – Graphic results without water cooling

Table 7.1 – Summary of the temperature of the thermal simulation on the concept 1.0, without any cooling media

Solid	T_{max} [°C]	T_{avg} [°C]
Support	284.5	176.5
Sensor	265	260
Epoxy	271	255

As it is possible to see in the Table 7.1, the temperatures reached without any cooling media/device are far away too big in rapport to the specification **Temperature**¹. The necessity of a cooling system is clear and mandatory.

¹relate to Chapter 3.1

7.1.2 With water in cooling pipe

In this simulation the water is approximated to a fixed temperature in the pipes. The constant temperature is T_{const} °C.

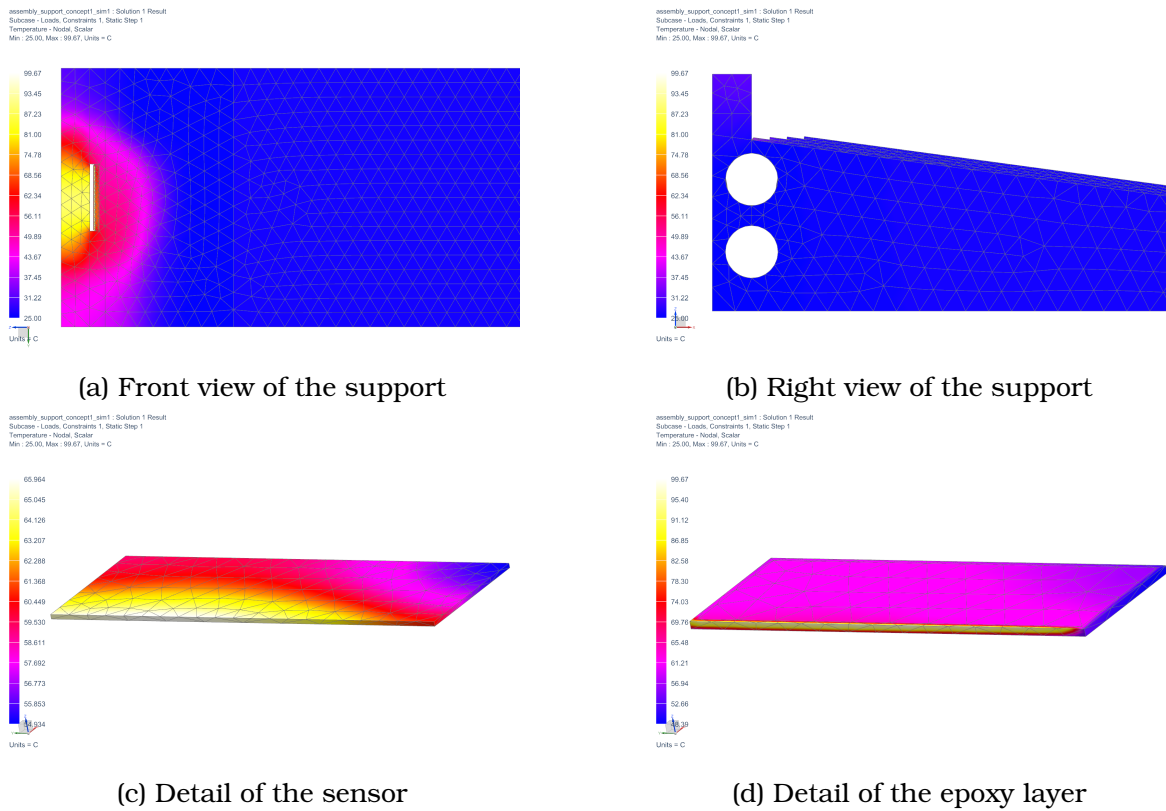


Figure 7.2 – Graphic results with water cooling at constant temperature

Table 7.2 – Summary of the temperature of the thermal simulation on the concept 1.0, with water at constant temperature

Solid	T_{max} [°C]	T_{avg} [°C]
Support	88.5	30.2
Sensor	66	60.6
Epoxy	99,7	64.1

7.1.3 Conclusion

Comparing the Tables 7.1 and 7.2 it is possible to see how the water cooling really affected the temperatures. In the case *with water cooling* the highest temperature is under **100 °C**. It is possible to make the conclusion that the cooling system using water will be effective and that the efforts for the upcoming simulations should go in that direction.

7.2 Simulations on concept 1.4

In order to approach the simulation of the water flow the simulation of the concept 1.4 has been done with the solver *NX THERMAL/FLOW*.

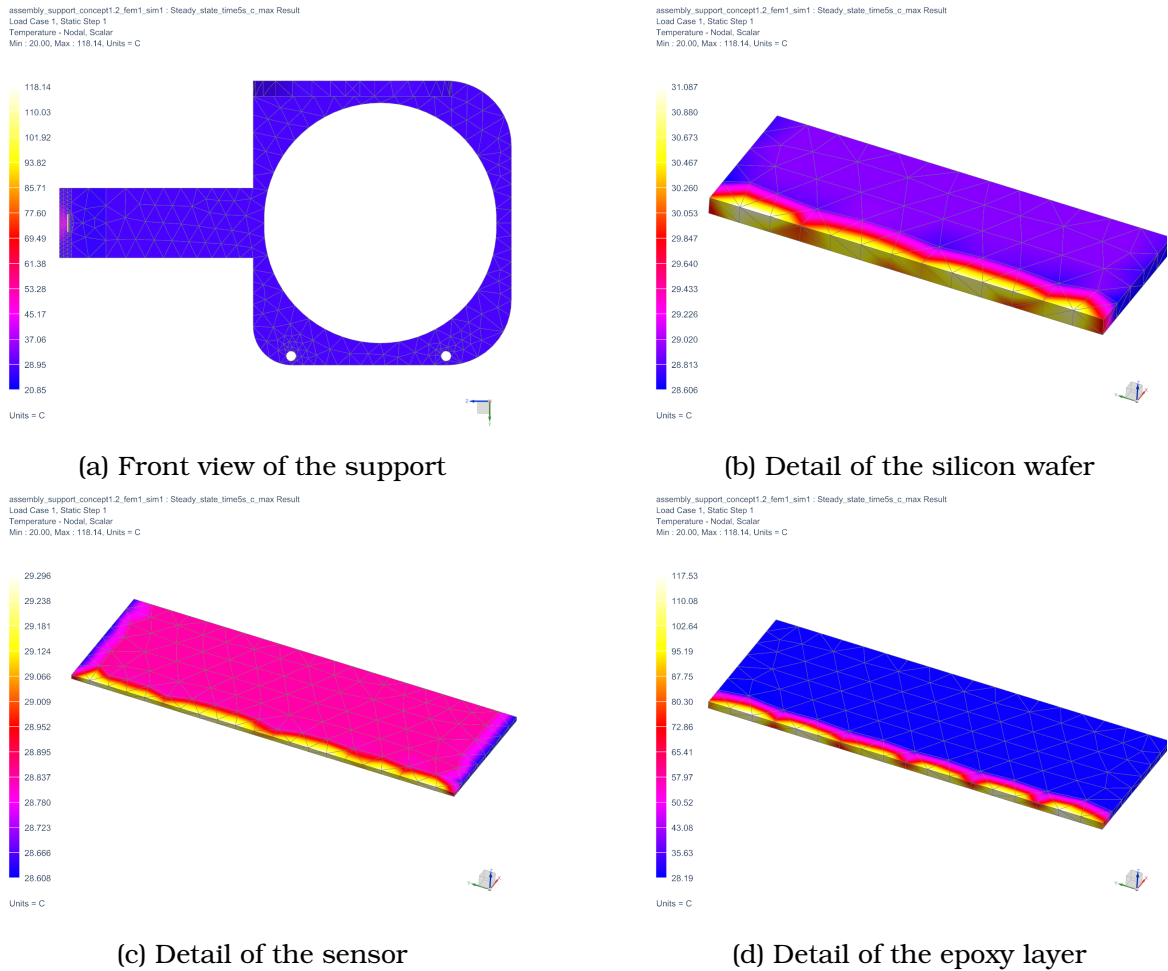


Figure 7.3 – Graphic results with water cooling, with water flow

Table 7.3 – Summary of the temperature of the thermal simulation on the concept 1.4, with water flow

Solid	T_{max} [°C]	T_{avg} [°C]
Support	42.3	26.6
Sensor	29.3	29.9
Epoxy	117.5	40.2
Wafer	31.1	29.1

The water flow graphic results are represented in the following Figure 7.4, as it is possible to see the temperature does not change significantly but the heat dissipation is better since the temperatures are much lower. In the Table 7.3 a summary of the water temperatures is shown.



Figure 7.4 – Graphic water heat evolution

Table 7.4 – Summary of the temperature of the thermal water flow simulation on the concept 1.4

Liquid	T_{max} [°C]	T_{avg} [°C]
Water flow	20.4	20.2

7.2.1 Conclusion

Taking a look at the Tables 7.2 and 7.3 and comparing the values it is possible to observe how in with the 1.4 concept and a continuous water flow the temperatures are significantly lower, the next simulations will be adjusted to the new concept design but keeping the same conditions tested at this point. The unique issue is the epoxy layer: the temperature of the volume near the face where the X-Ray beam hits it is really hot (99.5 °C for the concept 1.0 and 117.5 °C for the 1.4) if compared to the rest of the elements of the support. The issue is due to the worst thermal capacities that the epoxy resin has, compared to those of the copper and silicon of the sensor and the wafer.

7.3 Simulations on concepts 1.6 and 1.7

Since the concepts 1.6 and 1.7 did not bring any improvement to the simulations their graphic detailed report will not be presented, anyhow in the Figure 7.5 the graphic overview is represented and in the Tables 7.5 and 7.6 the main thermal values are summarized.

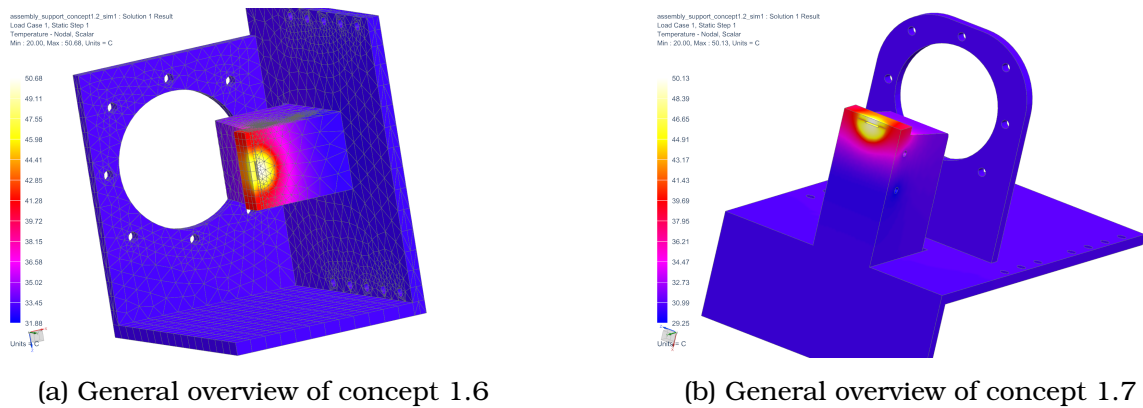


Figure 7.5 – General graphic results of concepts 1.6 and 1.7

Table 7.5 – Summary of the temperature of the thermal simulation on the concept 1.6

Solid	T_{max} [°C]	T_{avg} [°C]
Support	50.7	34.4
Sensor	44.0	42.5
Epoxy	98.5	40.2
Wafer	44.3	44.5

Table 7.6 – Summary of the temperature of the thermal simulation on the concept 1.7

Solid	T_{max} [°C]	T_{avg} [°C]
Support	50.1	37.4
Sensor	47.9	47.9
Epoxy	95.5	44.2
Wafer	49.5	47.9

7.4 Simulation on concept 1.8

In this section the thermal simulations with the *NX THERMAL/FLOW* solver are made on the last concept developed. The results of this last simulation combined with the previous results will be used in the Chapter 8 to achieve the best design possible. The graphic overview visible at the Figure 7.6 show how does the heat transfer behaves in the complete support.

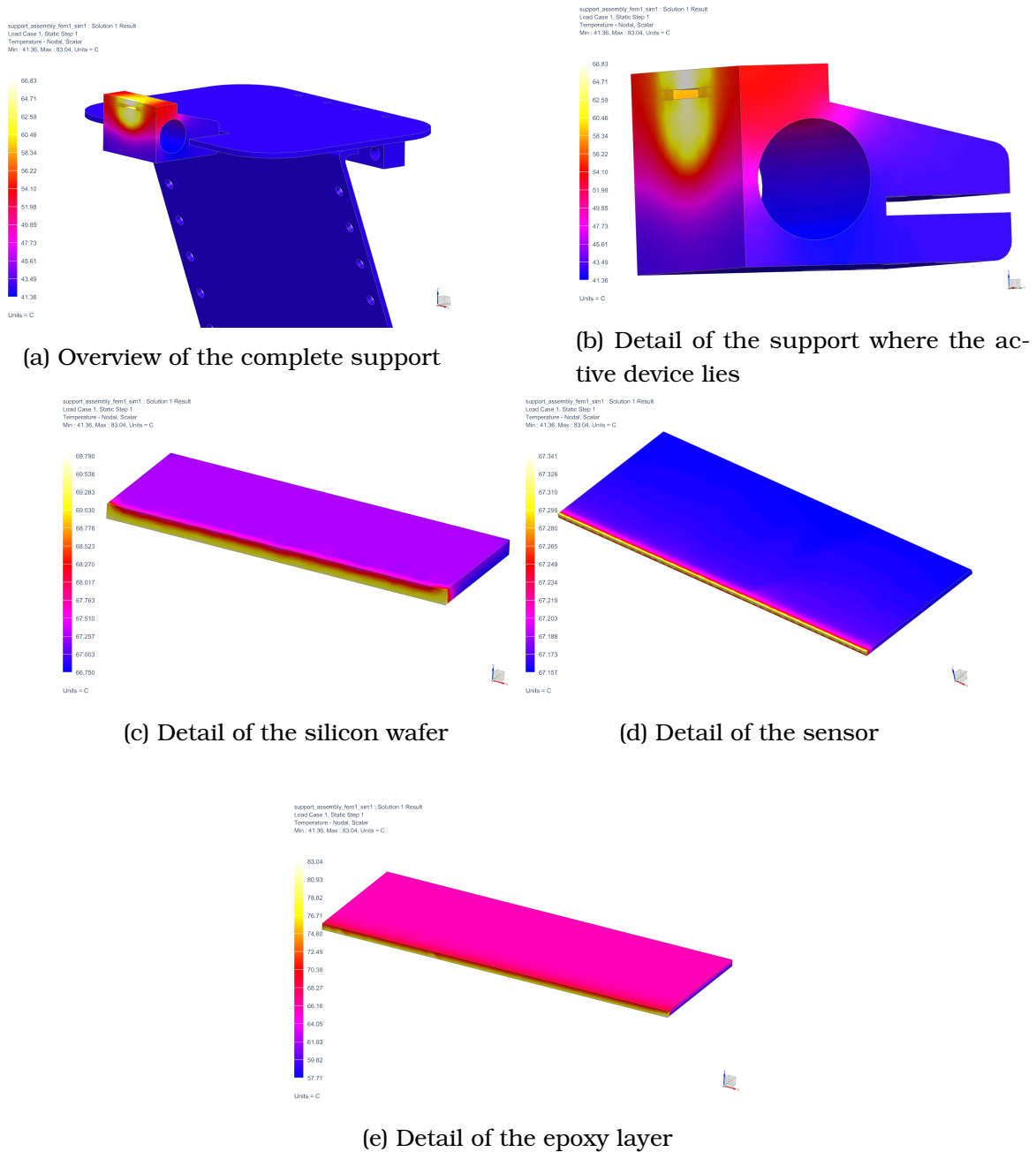


Figure 7.6 – Graphic results for the simulation of concept 1.8 12.7 mm pipe

Table 7.7 – Summary of the temperature of the thermal simulation on the concept 1.8 with the 12.7 mmpipe

Solid	T_{max} [°C]	T_{avg} [°C]
Support	66.8	43.5
Support detail	66.8	49.4
Sensor	67.3	67.2
Epoxy	83.0	66.9
Wafer	69.8	67.3

In the Table 7.7 it is possible to see the summary of the temperatures in the various elements composing the concept 1.8, comparing these temperatures with the temperatures that can be found in the previous Tables it can be notice how the results are globally worse. The epoxy layer is as like in every previous simulation the element which is more heated.

7.5 Conclusions

With the results of these simulations it is now possible to proceed to the improvement of the design of the concept 1.8. The main problems that have been found are:

- the epoxy layer temperature has to be reduced
- the global temperature has to be lowered as more as possible
- mass has to be decreased

In the following chapter: **Improvements** those problems would be analysed and solved.

Chapter 8

Improvements

The goal of this chapter is to take advantage of the results of the simulation from the previous Chapter 6 and adjust the design in order to solve the problems. At the end one final design will be provided.

8.1 Epoxy overheating

The epoxy overheating is a bigger issue because it is in direct contact with the silicon wafer and the contact between the two could lead to an overheating of the wafer and consequently of the sensor. In order to prevent this overheating it has been decided to put a "shield" in front of the epoxy layer, the shield will be made out of copper. The minimal thickness needed to absorb the 100% of the energy of the radiations is determined in the Appendix A.3 and is COMPLETEARE

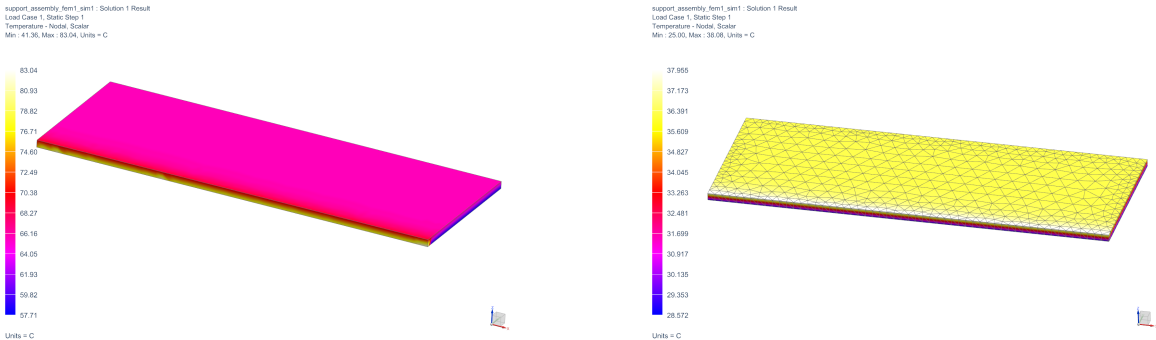


Figure 8.1 – Thermal results on the epoxy layer without and with the shield absorbing the radiations

As it can be observed in the Table 8.1 the diminution of temperature is important: the temperature drops from 83°C to 38°C. In conclusion the shield is really effective in protecting the epoxy layer from a direct radiation and will be implemented in the future design.

Table 8.1 – Comparison between temperatures

Shield present	T_{max} [°C]	T_{avg} [°C]
NO	83.0	66.9
YES	38.0	30.8

8.2 Global temperature

8.2.1 First iteration: diminution of the pipe diameter

More the global temperature will be low and more the sensor and the boards will be safe. In order to try to increase the heat dissipation through the water the pipes have been modified: the diameter is in this step 6 mm, this diameter will increase the speed of the water flow, the increase of speed will increase the turbulent nature of the flow in the pipe and consequently the heat exchange should be better.

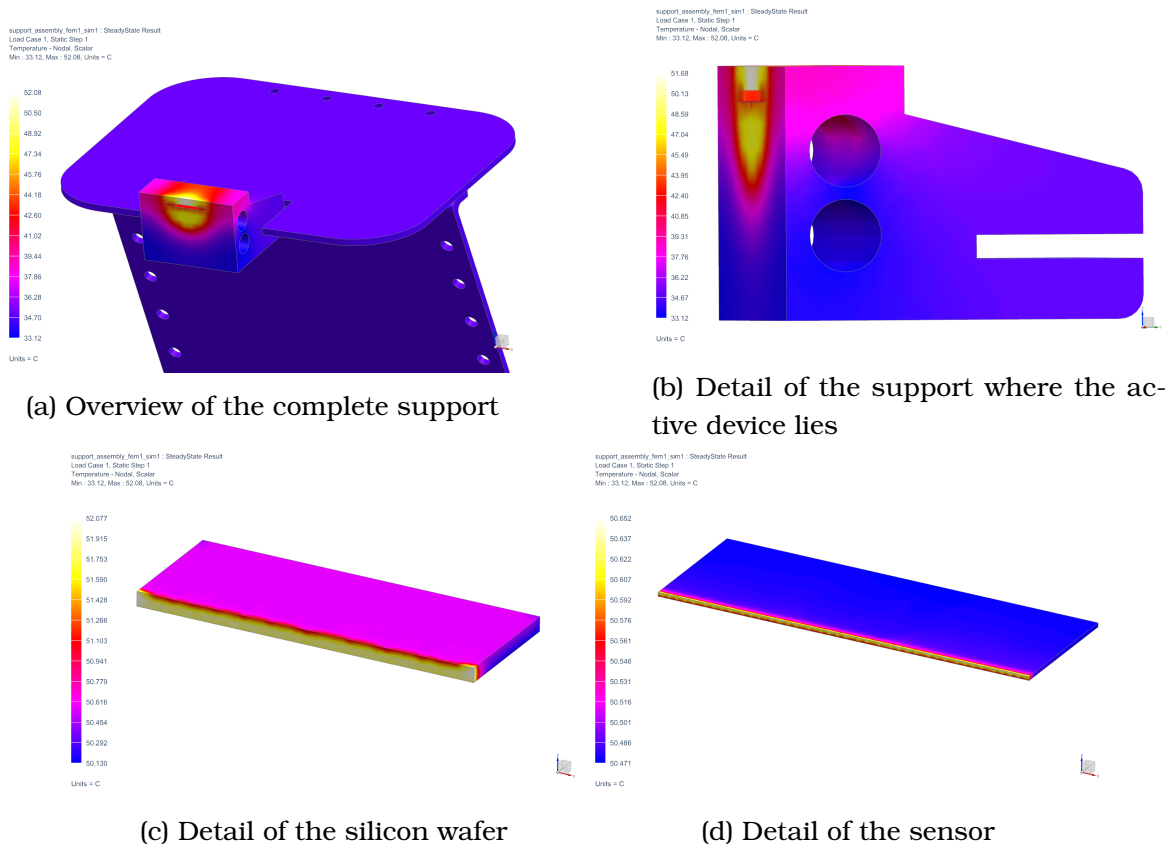


Figure 8.2 – Graphic results for the simulation of concept 1.8 with the 6 mm pipe

Table 8.2 – Summary of the temperature of the thermal simulation on the concept 1.8 with the 12.7 mm pipe

Solid	T_{max} [°C]	T_{avg} [°C]
Support	66.8	43.5
Support detail	66.8	49.4
Sensor	67.3	67.2
Epoxy	83.0	66.9
Wafer	69.8	67.3

Table 8.3 – Summary of the temperature of the thermal simulation on the concept 1.8 with the 6 mm pipe

Solid	T_{max} [°C]	T_{avg} [°C]
Support	51.7	35.5
Support detail	51.7	38.8
Sensor	50.7	50.5
Epoxy	52.0	44.8
Wafer	52.1	50.5

The global temperature is decreased, comparing the Tables 8.2 and 8.3 it is possible to see how the double pipe is more effective and how the temperature between the different elements are now similar.

8.2.2 Second iteration: changing the pipe position

However in the Figure 8.2(b) it is possible to see how the lower pipe is not too much effective, moving this pipe closer to the upper wall of the support could make it more effective:

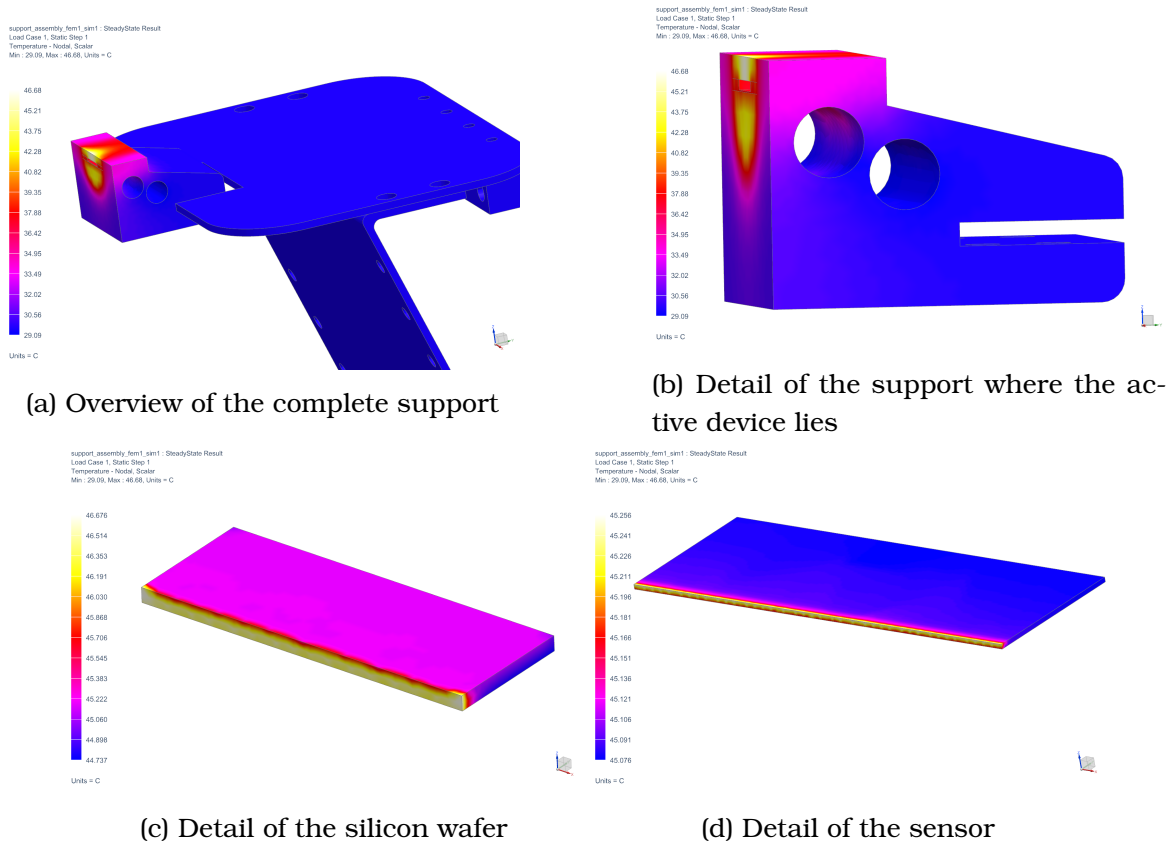


Figure 8.3 – Graphic results for the simulation on the improvements of concept 1.8 with the 6 mm pipe

Table 8.4 – Summary of the temperature of the thermal simulation on the improvements of the concept 1.8 with the 6 mm pipe

Solid	T_{max} [°C]	T_{avg} [°C]
Support	51.7	35.5
Support detail	45.3	38.8
Sensor	45.3	45.1
Epoxy	46.5	43.6
Wafer	46.7	45.2

Table 8.5 – Summary of the temperature of the thermal simulation on the concept 1.8 with the 12.7 mm pipe

Solid	T_{max} [°C]	T_{avg} [°C]
Support	66.8	43.5
Support detail	66.8	49.4
Sensor	67.3	67.2
Epoxy	83.0	66.9
Wafer	69.8	67.3

Effectively the results of this second iteration (Table 8.4) are better than the those from the concept 1.8 (Table 8.5). Due to the presence of two type of pipe (12.7 mm and 6 mm diameter) in the KEK Facility the iterations in this direction ends here.

8.3 Mass reduction

The goal of this section is to reduce as possible the mass of the complete support. The reduction will be made by extruding pockets in the support, those pockets will affect the stiffness of the structure. To control that the structure remains rigid the *NX NASTRAN Static Load* solver will be used.

8.3.1 First iteration: determination of actual stiffness

Instead of determinate the stiffness of the structure the displacements will be judged, the first operation is to create a FEA model of the support and to apply the initial conditions. The condition are two:

1. displacements blocked on the flange
2. static load of 10 N to simulate the weight of the whole support imposed on the furthest edge of the electronic support plate

In the Figure 8.4 it is possible to see those two conditions applied:



(a) Overview of the fixed conditions (in blue)

(b) Overview of the force emplacement (in red)

Figure 8.4 – Limit conditions applied to the structure for the static load simulation

In the Figure 8.5 the results of the static load simulation are presented, it is possible to see how the point where the force has been applied is the point with the biggest displacement: 0.3 mm but this point does not represents something interesting. It is necessary to look at the point where the sensor will be positioned, in this point the displacement is 0.03 mm and is this displacement that has to be kept at the minimum possible. A maximal allowed displacement of 0.1 mm has been imposed.

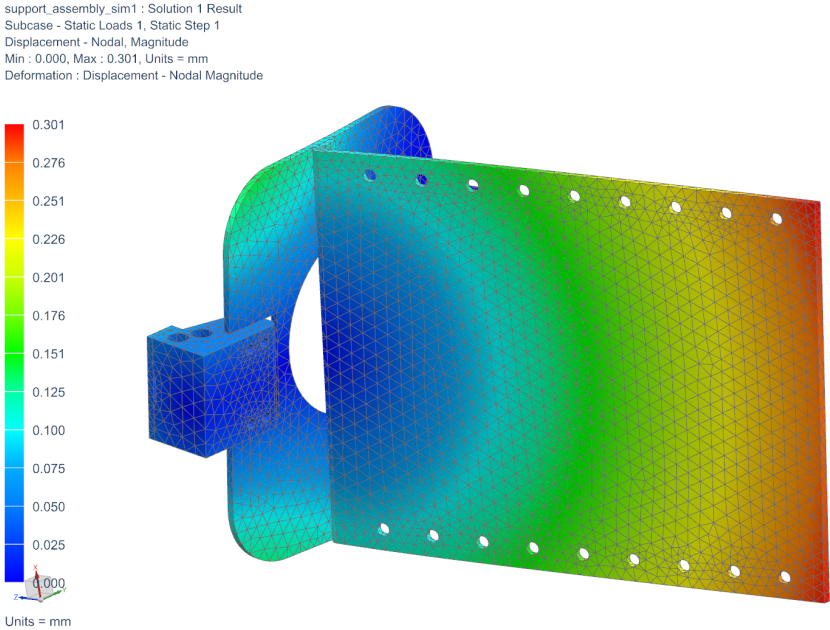


Figure 8.5 – Displacement of the support

8.3.2 Second iteration: creating the new model and simulation

As said before, the easiest way to reduce the mass is to subtract pockets in the electronic support plates. In the Figure 8.6(a) the new concept already meshed is represented, the fixed initial conditions are applied at the same flange but the force is now applied in the last hole of the electronic support plate(Figure 8.6(b)).

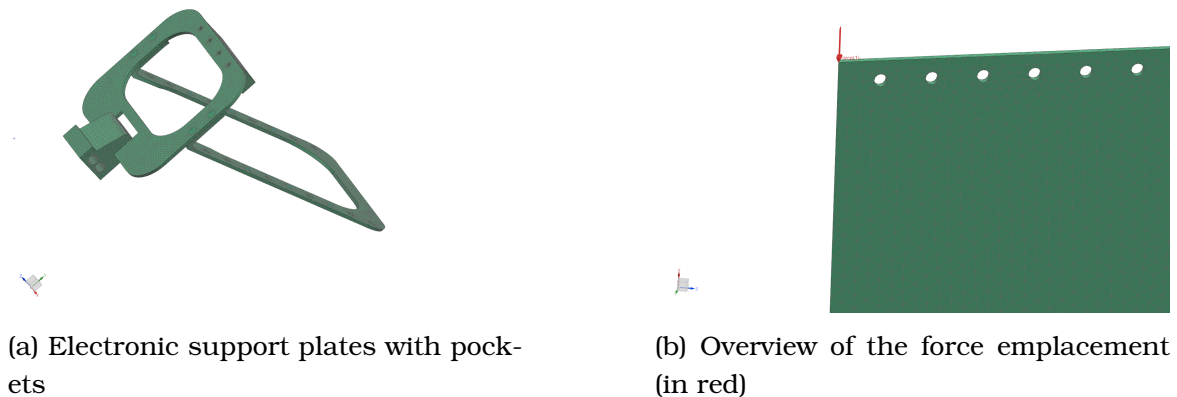


Figure 8.6 – Limit conditions applied to the structure for the static load simulation

The results of this simulations are presented in the Figure 8.7, the point where the force is applied is this time too the point with the major displacement: 0.8 mm. Anyway the area where the sensor will be glued has a maximal displacement of **0.07 mm**, which is under the displacement chosen as maximal.

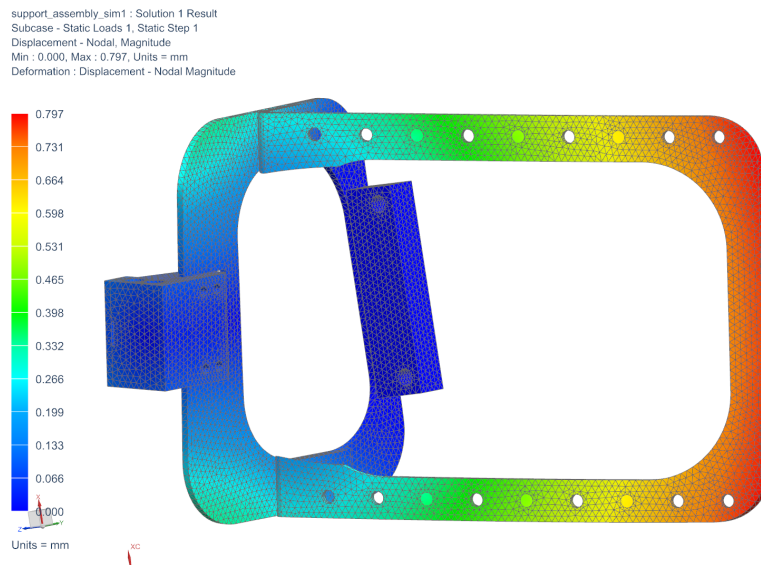


Figure 8.7 – Displacement of the support

The mass of the support is now $m_s = 379.9$ g which gives a total mass of $m_{tot} = 999$ g! The **mass** specification is now respected.

Chapter 9

Conclusions

9.1 Synthesis and final design

After being introduced to the BELLE2 experiment and the X-Ray characterization the project started quickly. In parallel with the 3D conception the FEA and the following simulations took place and helped the conception of a lightweight support, in the Figure 9.1 it is possible to see what is the final results after all the design iterations.

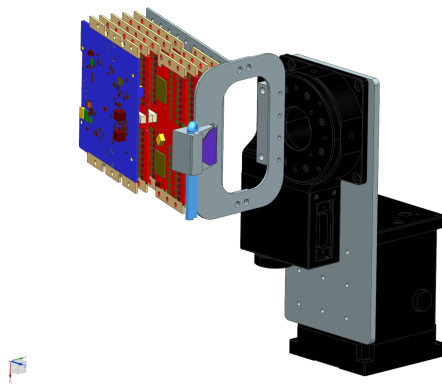


Figure 9.1 – Final 3D design

The many feedbacks from different persons really helped to fast understand the difficulties of working with really small parts in such a delicate environment. The design of the perfect mount is far from being achieved but this thesis has provided a solid base to start from. The thermal simulations that have been made showed how a liquid cooling device was needed, the subsequent implementation of the water cooling and the flow characterization helped to reach the best heat dissipation possible. The following step of the simulations should be the implementation of the pure Helium atmosphere in order to take in count the convection of the support with the gas, this could improve the heat dissipation. Even if the Design Specifications have been completely fulfilled there is still work to do in order to perfect the simulations and optimize the mass.

9.2 Recommendations

First of all, in order to reduce weight and keep stiffness at an acceptable level it could help to pass the geometry through an optimization process with the dedicated tool which is present in NX SIEMENS 10. This tool allows to impose which constrain has to be respected and what geometry we want to change in order to find the best combination. It is necessary to evaluate the danger of the beam accidentally hitting the electronic boards, a shield could easily be added to the structure but in that case the weight will increase. Another way to reduce weight will be the research for plastics or composite materials, since plastics is largely used in the electronic supports it will not be difficult to find the perfect combination between size, mass and price. One good candidate for the electronic support is PEEK, this material finds its applications in the electronic domain, it is easily machinable but has a higher price (**90 USD for one kg**).

Declaration of Authorship

I, RINALDI Fabio, declare that this thesis titled, *Design of a Mount for a new generation X-Ray Detector Board* and the work presented in it are my own. I confirm that:

- This work was done wholly or mainly while in candidature for a research degree at this University.
- Where any part of this thesis has previously been submitted for a degree or any other qualification at this University or any other institution, this has been clearly stated.
- Where I have consulted the published work of others, this is always clearly attributed.
- Where I have quoted from the work of others, the source is always given. With the exception of such quotations, this thesis is entirely my own work.
- I have acknowledged all main sources of help.
- Where the thesis is based on work done by myself jointly with others, I have made clear exactly what was done by others and what I have contributed myself.

Signed:

Date: July 29, 2016

Appendices

Appendix A

Calculations

This appendix is dedicated to all the manual calculations that were made during this project.

A.1 Heat Transfer

An attempt to determine manually the heat transfer through the sensor has been done, unfortunately it has not been possible to establish how much will the radiations heat the target face, anyhow here it is possible to find some calculations that helped putting the simulations in the right way:

$$Bi = \frac{\alpha \cdot L_c}{\lambda}$$

with: $L_c = 2.415mm$, $\alpha = 5W/(m^2 \cdot K)$ and $\lambda = 400W/m \cdot K$ we have a Bi of:

$$Bi = 3.0187 \cdot 10^{-5} < 0.1$$

if $Bi < 0.1$ the solid final temperature will be homogeneous and the **global capacity method is therefore applicable**.

$$\tau = \frac{\rho \cdot L_c \cdot c_p}{\alpha}$$

with: $L_c = 2.415mm$, $\alpha = 5W/(m^2 \cdot K)$, $\rho = 8900kg/m^3$, $c_p = 385J/kg \cdot K$:

$$\tau = 1655$$

τ represent the time limit from which the system analysed reached the steady state, the thermal conditions will not change any more.

A.2 Flow Characteristics

In order to characterize the flow conditions the following equation were used and implemented in an excel spreadsheet to simplify the calculations

$$Re = \frac{\rho \cdot d_p \cdot \dot{v}}{\eta A_s}$$

In the following Figure A.1(a) it is possible to have an overview over the different Reynolds numbers calculated, it is important to remember that a flow is considered completely turbulent when the Reynolds number is over 4000, in the Figure A.1(b) it is possible to see which are the minimal volumic flow rate to achieve the turbulence:

v[l/min]]	c[mm/s]	d[mm]	r[mm]	As[mm2]	Nu[mm2/s]	Re
5	11789	3	1.5	7.1	1.1	32153
	6631	4	2	12.6		24114
	4244	5	2.5	19.6		19292
	2947	6	3	28.3		16076
	2165	7	3.5	38.5		13780
	1658	8	4	50.3		12057
	1310	9	4.5	63.6		10718
	1061	10	5	78.5		9646
	877	11	5.5	95.0		8769
	658	12.7	6.35	126.7		7595

(a) Different Reynolds numbers calculated for different pipe diameter at the given flow

Re	Nu [mm2/s]	d[mm]	r[mm]	As[mm2]	c[mm/s]	v[l/min]
4000	1.1	3	1.5	7.1	1467	0.62
		4	2	12.6	1100	0.83
		5	2.5	19.6	880	1.04
		6	3	28.3	733	1.24
		7	3.5	38.5	629	1.45
		8	4	50.3	550	1.66
		9	4.5	63.6	489	1.87
		10	5	78.5	440	2.07
		11	5.5	95.0	400	2.28
		12.7	6.35	126.7	346	2.63

(b) Different volume flow rates calculated for a Re= 4000

Figure A.1 – Water flow characterization

A.3 X-Ray penetration in the matter

The beam penetration in the copper support has been calculated with the following equation

$$I_x = I_0 \cdot e^{-\mu \cdot \rho}$$

I_x is the energy of the beam at the x distance from the surface I_0 is the initial energy of the beam hitting the surface target μ is a tabular valor for the mass attenuation of X-Rays in Copper, it depends from the energy of the beam and the volumic mass of copper, in this case with a peak of 20keV has been found to be 300.7.

The penetration has been calculated for when the energy is zero, the result is **4,85 mm**. The security thickness selected for the shield is **5 mm**.

A.4 couple on the rotational stage

The couple that the rotational stage will manage has been calculated with the following equations:

$$M = F \cdot d$$

$$F = 10 \text{ N}$$

$$d = 0.198 \text{ m}$$

The couple that will act on the rotational stage is in the worst of the cases **1.98 Nm**

Appendix B

Positioning motors data-sheets

Motion Control Products

RoHS
CE

Rotation Motorized Stages | SGSP-YAW

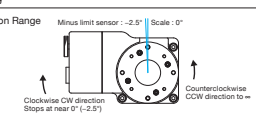


Stepping motor driven rotation stages fitted with bearing guide and worm gear feed mechanism.

- Motorized stages suitable for positioning for measuring, inspection and evaluation instruments.

Guide

▶ **Rotation Range**



▶ Homing of rotation motorized stages is performed with the CW limit sensor as the origin sensor.

▶ Origin detection is adjusted so that the stage stops at 0 degree when homing is performed in the MINI system at half step.

Attention

▶ Attention is required when mounting in upside down orientation or on a vertical plane.

▶ Precision and load capacity specifications may be partly not satisfied depending on the mounting orientation.

Specifications						
Part Number		SGSP-80YAW	SGSP-120YAW	SGSP-160YAW	SGSP-120YAW-W	
Mechanical Specifications	Rotation Range	Move in the counterclockwise CCW direction to ∞, and stop at near 0 degree (-2.5°) in the clockwise CW direction.				
	Table Size [mm]	φ80	φ120	φ160	φ120	
	Travel Mechanism (reduction ratio)	Worm gear (1:144)	Worm gear (1:144)	Worm gear (1:144)	Worm gear (1:144)	
	Positioning Slide	Bearing method	Crossed roller	Crossed roller	Crossed roller	
	Stage Material	Aluminum / Aluminum bronze	Aluminum / Aluminum bronze	Aluminum / Aluminum bronze	Aluminum / Aluminum bronze	
Accuracy Specifications	Weight [kg]	1.1	2.0	2.5	5.5	
	Resolution	(Full) [°/pulse]	0.005	0.005	0.005	0.005
		(Half) [°/pulse]	0.0025	0.0025	0.0025	0.0025
	MAX Speed [°/sec]	30	30	30	30	
	Positioning Accuracy [°]	0.15	0.1	0.1	—	
	Positional Repeatability [°]	0.02	0.02	0.02	0.02	
	Load Capacity [N]	98 (10.0kgf)	196 (20.0kgf)	196 (20.0kgf)	196 (20.0kgf)	
	Moment Stiffness [°/N-cm]	0.2	0.1	0.1	—	
	Lost Motion [°]	0.05	0.05	0.05	—	
	Backlash [°]	0.08	0.08	0.08	0.08	
Sensor	Parallelism [μm]	50	50	60	—	
	Concentricity [μm]	30	30	30	—	
	Wobble [mm]	0.02	0.02	0.02	—	
	Sensor Part Number	Micro Photoelectric Sensor: PM-F24 (SUNX Co., Ltd.)				
Limit Sensor	Equipped (NORMAL CLOSE)	Equipped (NORMAL CLOSE)	Equipped (NORMAL CLOSE)	Equipped (NORMAL CLOSE)		
Origin Sensor	None	None	None	None		
Proximity Origin Sensor	None	None	None	None		

Motor / Sensor Specifications		
Motor	Type	5-phase stepping motor 0.75A/phase (Oriental Motor Co., Ltd.)
	Motor Part Number	C865-80215P (∅28mm)
	Step Angle	0.72°
Sensor	Power Voltage	DC5 - 24V ±10%
	Current Consumption	15mA or lower
	Control Output	NPN open collector output DC30V or lower, 50mA or lower
	Output Logic	When shaded: Output transistor OFF (no conduction)

Compatible Driver / Controller	
Control System	Compatible Driver SG-5M, SG-5MA, SG-55M, SG-55MA, SG-514MSC, SG-5151, KR-S25M
Compatible Controller	SHOT-702, GIP-101, SHOT-302GS, SHOT-304GS, HIT-M/HIT-S

Figure B.1 – Rotational stage data sheet

Motion Control Products

Translation Motorized Stages, Flat Z axis - 5 Phase Stepping Motor

SGSP-ZF Stage size □40/□60/□80mm

RoHS

Z axis stepping motor driven stages for measurement and inspection, offering high stiffness and high precision.
The table that travels up and down is horizontal and offers smooth travel.



- Originally designed horizontal plane Z axis stages in which a motor is incorporated in its main body for space-saving.
- Minimized protrusions make these stages ideal for system assembly.

Attention

- ▶ The SGSP40-5ZF is fixed at three points.

Specifications		SGSP40-5ZF	SGSP60-5ZF	SGSP60-10ZF	SGSP80-20ZF	
Part Number						
Mechanical Specifications	Travel [mm]	5	5	10	20	
	Table Size [mm]	40×40	60×60	60×60	80×80	
	Feed Screw [mm]	Ball screw diameter φ5mm, 1mm lead	Ball screw diameter φ6mm, 1mm lead	Ball screw diameter φ6mm, 1mm lead	Ball screw diameter φ8mm, 2mm lead	
	Positioning Slide	Outer rail structure	Outer rail structure	Outer rail structure	Outer rail structure	
	Stage Top Material	Aluminum	Aluminum	Aluminum	Aluminum	
	Finish	Black anodized	Black anodized	Black anodized	Black anodized	
	Weight [kg]	0.35	0.6	0.6	1.6	
Accuracy Specifications	Resolution	(Full) [μm/pulse]	1.0	2.0	2.0	0.2
		(Half) [μm/pulse]	0.5	1.0	1.0	0.1
	MAX Speed [mm/sec]	2	4	4	2	
	Positional Repeatability [μm]	10	10	10	10	
	Load Capacity [N]	19.6 (2.0kgf)	39.2 (4.0kgf)	39.2 (4.0kgf)	147 (15.0kgf) ^{*1}	
	Moment Stiffness	Pitch [°/N-cm]	2.0	0.4	0.4	0.2
		Yaw [°/N-cm]	2.0	1.0	1.0	1.0
		Roll [°/N-cm]	1.0	1.0	1.0	1.0
	Lost Motion [μm]	5	5	5	5	
	Parallelism [μm]	50	50	50	50	
Running Parallelism [μm]	15	15	15	15		
Pitch [°]	25	20	20	25		
Sensor	Sensor Part Number	Micro photo sensor: EE-SX4134 (OMRON Corporation); Limit sensor, origin sensor Micro photo sensor: PM-U24 (SUNX Co., Ltd.); Silt origin sensor				
	Limit Sensor	Equipped (NORMAL CLOSE)	Equipped (NORMAL CLOSE)	Equipped (NORMAL CLOSE)	Equipped (NORMAL CLOSE)	
	Origin Sensor	None	None	None	None	
	Proximity Origin Sensor	None	None	None	None	

^{*1} If you use a controller or driver with a mark of ②.

Motor / Sensor Specifications					
Motor	Type	5-phase stepping motor 0.35A/phase (Oriental Motor Co., Ltd.)		5-phase stepping motor 0.75A/phase (Oriental Motor Co., Ltd.)	
	Motor Part Number	PK513PB-C9 (□20mm)	C9863-90215P (□28mm)	C9863-90215P (□28mm)	PMM33BH-MG20 (□28mm)
	Step Angle	0.72°			
Sensor	Power Voltage	DC5 - 24V ±10% or lower			
	Current Consumption	30mA or lower (15mA or lower per sensor)			
	Control Output	NPN open collector output DC30V or lower, 50mA or lower			
	Output Logic	When shaded: Output transistor OFF (no conduction)			

Compatible Driver / Controller			
Control System	Compatible Driver	SG-5MA, SG-55MA	①: SG-5M, SG-5MA ②: SG-55M, SG-55MA, SG-514MSC, SG-5151, KR-525M
	Compatible Controller	①: GSC-01, SHOT-102, GSC-02 ②: SHOT-702, SHOT-302GS, SHOT-304GS, HIT-M/HIT-S	

1056

Figure B.2 – Translational stage data sheet

List of Figures

1	Vue isométrique du concept 1.0	ii
2	Résultat de la simulation thermique faite sur le support final	ii
3	Vista isometrica del concetto 1.0	iii
4	Risultati della simulazione termica sul supporto finale	iii
5	Isometric view of concept 1.0	iv
6	Results for final support thermal simulations	iv
1.1	KEK facility layout	1
1.2	The X-Ray entering the box through an orifice, side note: the picture has been taken without external light source...	2
3.1	Overview of the actual installation	5
4.1	Sensor layout and dimensions	6
4.2	Sensor 3D model	7
4.3	Overview of the support of the concept 1.0	8
4.4	Isometric view of the first concept	8
4.5	Sensor position	9
4.6	Sensor in working position	9
4.7	Isometric view of concept 1.4	10
4.8	Front and right views of the concept 1.4	10
4.9	Mass determination of 2 amplifier boards	11
4.10	Details of the balance, precision stated at 0.1 g	11
4.11	Trimetric view of concept 1.6	12
4.12	Left and right views of the concept 1.6	12

4.13	Sensor position	13
4.14	Isometric view of 1.7 concept	14
4.15	Upper and right views of the concept 1.7	14
4.16	Flexible cables for signal transmission	15
4.17	Isometric view of concept 1.8	16
4.18	Upper view of concept 1.8	17
4.19	The two active device supports, the hole has the same size: $d_h = 12.7 \text{ mm}$	18
5.1	Mesh of the sensor	19
5.2	Mesh of the wafer	20
5.3	Mesh of the epoxy layer	20
5.4	Mesh of the support for the electronic boards	20
5.5	Mesh of the plate	21
5.6	Mesh of the flange	21
5.7	Mesh of the internal diameter of the pipe	21
5.8	Mesh of the active device support	22
5.9	Subdivision of the support, in order to separate the beam action area	22
6.1	Simulation Contacts between surfaces	23
6.2	Application of the initial temperature to the complete support	24
6.3	Application of the initial temperature to the water	24
6.4	Application of the initial temperature and initial flow volume rate to the water	25
6.5	Application of the heat flux as load	25
7.1	Graphic results without water cooling	28
7.2	Graphic results with water cooling at constant temperature	29
7.3	Graphic results with water cooling, with water flow	30
7.4	Graphic water heat evolution	31
7.5	General graphic results of concepts 1.6 and 1.7	32
7.6	Graphic results for the simulation of concept 1.8 12.7 mm pipe	33
8.1	Thermal results on the epoxy layer without and with the shield absorbing the radiations	35

- 8.2 Graphic results for the simulation of concept 1.8 with the 6 mm pipe 36
- 8.3 Graphic results for the simulation on the improvements of concept 1.8 with
the 6 mm pipe 38
- 8.4 Limit conditions applied to the structure for the static load simulation 40
- 8.5 Displacement of the support 40
- 8.6 Limit conditions applied to the structure for the static load simulation 41
- 8.7 Displacement of the support 41

- 9.1 Final 3D design 42

- A.1 Water flow characterization 47

- B.1 Rotational stage data sheet 50
- B.2 Translational stage data sheet 51

List of Tables

1	List of acronyms used	v
2	List of materials used	v
3	Mathematical constants	vi
7.1	Summary of the temperature of the thermal simulation on the concept 1.0, without any cooling media	28
7.2	Summary of the temperature of the thermal simulation on the concept 1.0, with water at constant temperature	29
7.3	Summary of the temperature of the thermal simulation on the concept 1.4, with water flow	30
7.4	Summary of the temperature of the thermal water flow simulation on the con- cept 1.4	31
7.5	Summary of the temperature of the thermal simulation on the concept 1.6 . .	32
7.6	Summary of the temperature of the thermal simulation on the concept 1.7 . .	32
7.7	Summary of the temperature of the thermal simulation on the concept 1.8 with the 12.7 mmpipe	34
8.1	Comparison between temperatures	36
8.2	Summary of the temperature of the thermal simulation on the concept 1.8 with the 12.7 mm pipe	37
8.3	Summary of the temperature of the thermal simulation on the concept 1.8 with the 6 mm pipe	37
8.4	Summary of the temperature of the thermal simulation on the improvements of the concept 1.8 with the 6 mm pipe	39
8.5	Summary of the temperature of the thermal simulation on the concept 1.8 with the 12.7 mm pipe	39

Bibliography

- [1] Instrumentation Development Lab web-page
http://www.phys.hawaii.edu/idlab/taskAndSchedule/_IDLtaskAndSchedule.html,
consulted between June 13, 2016 and July 29, 2016

- [2] NX NASTRAN, Thermal Analysis
http://www.plm.automation.siemens.com/en_us/products/nx/for-simulation/thermal-analysis/index.shtml,
consulted between June 13, 2016 and July 29, 2016

- [3] Physics constant for beam penetration
<http://physics.nist.gov/PhysRefData/XrayMassCoef/ElemTab/z29.html>,
consulted between June 13, 2016 and July 29, 2016

- [4] John R. Brauer,
What Every Engineer should know about Finite Element Analysis, William H. Middendorf,
University of Cincinnati, 1993

- [5] Mike Chainyk,
MSC/NASTRAN Thermal Analysis, The MacNeal.Schwendler Corporation, Los Angeles,
1994